
Prenatal and postnatal effects of gestational immune activation on synaptic and neurodevelopmental pathways via epigenetic mechanisms

Received: 27 June 2025

Revised: 18 December 2025

Accepted: 29 January 2026

Cite this article as: Zhu, B., Li, G., Saunders, J.M. *et al.* Prenatal and postnatal effects of gestational immune activation on synaptic and neurodevelopmental pathways via epigenetic mechanisms. *Transl Psychiatry* (2026). <https://doi.org/10.1038/s41398-026-03884-z>

Bohan Zhu, Gaoshan Li, Justin M. Saunders, Lynette B. Naler, Thomas M. Hadlock, Chenlong Wang, Adolfo García-Sastre, Javier González-Maeso & Chang Lu

We are providing an unedited version of this manuscript to give early access to its findings. Before final publication, the manuscript will undergo further editing. Please note there may be errors present which affect the content, and all legal disclaimers apply.

If this paper is publishing under a Transparent Peer Review model then Peer Review reports will publish with the final article.

Prenatal and postnatal effects of gestational immune activation on synaptic and neurodevelopmental pathways via epigenetic mechanisms

Bohan Zhu^{1,8}, Gaoshan Li^{1,8}, Justin M. Saunders², Lynette B. Naler¹, Thomas M. Hadlock¹, Chenlong Wang¹, Adolfo García-Sastre^{3,4,5,6,7}, Javier González-Maeso^{2,*}, Chang Lu^{1,*}

¹Department of Chemical Engineering, Virginia Tech, Blacksburg, VA 24061, USA.

²Department of Pharmacology and Toxicology, Virginia Commonwealth University School of Medicine, Richmond, VA 23298, USA.

³Department of Microbiology and Global Health & Emerging Pathogens Institute, Icahn School of Medicine at Mount Sinai, New York, NY 10029, USA.

⁴Department of Medicine – Division of Infectious Diseases, Icahn School of Medicine at Mount Sinai, New York, NY 10029, USA.

⁵The Tisch Cancer Institute, Icahn School of Medicine at Mount Sinai, New York, NY 10029, USA.

⁶The Icahn Genomics Institute, Icahn School of Medicine at Mount Sinai, New York, NY 10029, USA

⁷Department of Pathology, Molecular and Cell-Based Medicine, Icahn School of Medicine at Mount Sinai, New York, NY 10029, USA.

⁸These authors contributed equally: Bohan Zhu, Gaoshan Li.

*Correspondence: javier.maeso@vcuhealth.org (J.G.-M.); changlu@vt.edu (C.L.)

Abstract

Epidemiological research suggests that maternal immune activation (MIA) during early gestation is a significant risk factor for neurodevelopmental and psychiatric disorders in offspring. Epigenetic factors and chromatin-related phenomena remain highly dynamic throughout prenatal and early postnatal development, offering a substrate through which environmental insults can exert lasting effects on gene regulation. Here, we used a mouse MIA model induced by infection with a mouse-adapted influenza A/WSN/33 (H1N1) virus to investigate the long-term molecular consequences of maternal infection on adult offspring. To separately assess prenatal and postnatal effects of MIA, we cross-fostered half of the pups from each influenza-infected or mock-treated dam at birth. We then profiled histone modifications (H3K27ac, H3K4me3) and transcriptome changes in neuronal nuclei isolated from the frontal cortex of adult offspring. Our results revealed considerable overlap between the prenatal and postnatal effects of MIA on enhancer activity, suggesting a sustained regulatory trajectory across developmental stages. Prenatal MIA was specifically associated with changes in gene regulatory elements related to forebrain and telencephalon development, while postnatal MIA primarily affected pathways involved in axonogenesis and synapse organization. Cross-species enrichment analysis further revealed that MIA-responsive enhancers and promoters are significantly enriched at GWAS loci for neuropsychiatric disorders. Together, these findings support a model in which MIA contributes to disease risk through enduring epigenetic reprogramming of gene regulatory networks in the developing brain.

Introduction

Brain development is a highly orchestrated process regulated by both genetic and environmental factors, and it remains particularly vulnerable to perturbations during early life stages¹⁻³. Environmental insults can profoundly alter developmental trajectories and increase the risk of neurodevelopmental disorders, including schizophrenia, autism spectrum disorder (ASD), and attention-deficit/hyperactivity disorder (ADHD)⁴⁻¹⁰. Among these environmental challenges, maternal infection during pregnancy has emerged as a major risk factor^{7, 11}. Seminal serological studies, such as the Prenatal Determinants of Schizophrenia (PDS) study^{12, 13}, established that prenatal infection is associated with an increased risk of schizophrenia in the offspring. Subsequent epidemiological research has strengthened this link, revealing that prenatal exposure to a wide variety of microbial pathogens, including viruses (influenza and rubella), bacteria (bronchopneumonia), and protozoa (*Toxoplasma gondii*), is associated with a higher incidence of psychotic and neurodevelopmental disorders in adulthood¹⁴⁻¹⁶.

Maternal immune activation (MIA) may serve as a priming event that sensitizes the developing brain to subsequent insults, thereby increasing susceptibility to psychiatric and neurodegenerative disorders^{17, 18}. The immune system plays essential regulatory roles in neurodevelopment, contributing to neural induction, synaptic refinement, plasticity and circuit formation through diverse molecular and cellular mechanisms^{2, 19}. Experimental models of MIA have demonstrated that immune perturbations during gestation can disrupt synaptic function and neurotransmission in offspring, impacting multiple neurotransmitter systems, including GABAergic, serotonergic, glutamatergic, dopaminergic, and cholinergic pathways^{7, 20-23}.

The frontal cortex governs executive, cognitive, and emotional regulation and continues to mature well into adolescence²⁴. Its prolonged developmental trajectory and extensive synaptic remodeling make it particularly sensitive to prenatal environmental disturbances²⁵. Disrupted maturation of frontal cortical circuits has been consistently associated with neurodevelopmental disorders such as schizophrenia, autism spectrum disorder, and attention-deficit disorder^{26, 27}.

Epigenetic mechanisms are increasingly recognized as key mediators of gene–environment interactions in neurodevelopmental disorders²⁸⁻³¹. Prior studies have identified MIA-associated dysregulation of DNA methylation in the brain, such as promoter hypermethylation of GABAergic synthetic enzyme genes *GAD1* and *GAD2*³². More recently, genome-wide bisulfite and hydroxymethylcytosine sequencing has revealed broad alterations in DNA methylation and

hydroxymethylation landscapes in the offspring prefrontal cortex following MIA, further supporting an epigenetic basis for long-term neuronal and behavioral changes³³. Histone modifications have also been implicated, though studies to date – largely based on immunoblot and ChIP-qPCR assays in bulk brain tissue samples – have identified only a limited number of genes with altered histone acetylation at promoter regions^{34, 35}. These approaches lack the resolution and breadth to capture genome-wide epigenomic changes, particularly in a cell-type-specific context.

Histone modifications, including histone H3 acetylation at lysine 27 (H3K27ac) and histone H3 trimethylation at lysine 4 (H3K4me3), play critical roles in epigenomic regulation; H3K27ac marks active enhancers, whereas H3K4me3 marks active promoters. Enhancers, in particular, are highly dynamic cis-regulatory elements involved in neurodevelopmental processes³⁶. The activity of promoters is also strongly associated with the genetic risk of psychiatric disorders³⁷. Compared to DNA methylation, which primarily reflects long-term gene silencing³⁸, histone modifications mark active regulatory states and provide mechanistic insight into transcriptional control³⁹. However, few studies have examined cell-type-specific genome-wide variations in covalent histone modifications within the frontal cortex of MIA offspring. For example, one prior study using H3K4me3 ChIP-seq assays and mRNA microarrays in adult cerebral cortex reported minimal epigenetic alterations⁴⁰, possibly due to the use of whole tissue homogenates and the limited focus on promoter regions and gene expression.

Over the past few years, the development of MIA models in animals has been essential for testing causality, identifying molecular mechanisms, and developing new diagnostic tools and therapeutics. Rodent models^{41–43} – and more recently non-human primate models^{44, 45} – have demonstrated the causal relationship between MIA during pregnancy and neuropathological and behavioral abnormalities consistent with various neurodevelopmental psychiatric disorders. However, most previous studies in rodent MIA models have relied on maternal injections with poly-(I:C)^{41, 46, 47} or LPS⁴⁸, which principally drive innate immune responses. In contrast, viral infections also engage adaptive immune responses, suggesting that poly-(I:C)- or LPS-based models may not fully capture the spectrum of immune activation relevant to human conditions⁴⁹. Furthermore, poly-(I:C) and LPS act, for the most part, through single Toll-like receptors – TLR3 and TLR4 – respectively; whereas pathogens like mouse-adapted influenza virus elicit a more broad immune response engaging TLRs and RIG-I-like receptors⁴¹.

To investigate the long-term impact of MIA on adult offspring's epigenetic and transcriptomic landscapes, we combined MOWChIP-seq⁵⁰⁻⁵² for low-input profiling of H3K27ac and H3K4me3 with SMART-seq2^{53, 54} for transcriptome analysis in neuronal nuclei of mouse frontal cortex, a brain region involved in processes related to cognition, perception, and mood⁵⁵. We modeled MIA by infecting pregnant mice with influenza virus and generated the first dataset capturing cell-type-specific epigenomic and transcriptomic dynamics in the frontal cortex of adult offspring. Recognizing that the effects of MIA extend beyond gestation, we incorporated cross-fostering assays to assess the contribution of postnatal maternal behavior. Our goal was to determine whether the observed dysregulations in the offspring's brain are driven primarily by prenatal immune activation, postnatal maternal care, or a combination of both.

Methods

Animals

Experiments were conducted in accordance with NIH guidelines and were approved by the Virginia Commonwealth University Animal Care and Use Committee. All efforts were made to minimize animal suffering and the number of animals used. Animals were housed on a 12 h light/dark cycle at 23 °C with food and water ad libitum.

Mouse viral infection

Infection of timed pregnant female mice was performed as previously reported^{21, 22}. Briefly, timed pregnant female CD1 mice were obtained from Charles River Laboratories. On day 9.5 of pregnancy, mice were anesthetized with ketamine/xylazine before intranasal (i.n.) inoculation with 5×10^3 plaque-forming units (pfu) of influenza A/WSN/33 (H1N1) virus in 50 µl of PBS. Mock-treated mothers were treated identically but were administered PBS. Our previous data indicate that infection with this sublethal dose of virus causes sickness behavior (lethargy, sleepiness, ruffled fur and lack of grooming), but loss of pregnancy is uncommon²¹. Day 9.5 of pregnancy was chosen because it is neurodevelopmentally equivalent to the end of the first trimester of human pregnancy⁵⁶, a critical period during which environmental insults produce a higher risk of schizophrenia and autism in human offspring⁵⁷. At weaning (postnatal day 21), offspring were separated from their biological or surrogate mothers and assigned to cages based on their prenatal and postnatal treatment conditions. Males and females were housed separately in groups of three to five. Animals were not randomly assigned to experimental groups. Group allocation was determined solely by their prenatal and postnatal treatment conditions. Experimenters were not blinded to group assignments. Randomization was used for determining the order of samples processed for RNA-seq and ChIP-seq. All subsequent experiments were conducted in adulthood (10 weeks of age). A total of seven independent cohorts (A-G) were evaluated. Each group included six mice. For each mouse tissue sample, two technical replicates were produced for each RNA-seq or ChIP-seq assay. No formal statistical sample-size estimation was performed. Six animals per group were used based on experimental feasibility.

Postnatal cross-fostering

Within 24 h of birth, approximately half of the offspring born to MIA and control dams were removed from the original mother and then placed with a surrogate rearing mother, housed with stepsiblings born to this surrogate (control or MIA) mother (Fig. 1).

Mouse brain samples

Adult male mice were sacrificed by cervical dislocation, and bilateral frontal cortices (bregma 1.90-1.40) were dissected and frozen at -80 °C until sample processing.

Nuclei isolation and sorting via FACS

Nuclei isolation was conducted using a published protocol^{58, 59}. All steps were conducted on ice, and all centrifugation was conducted at 4°C. One piece of mouse frontal cortex tissue (6-10 mg) was placed in 3 mL of ice-cold nuclei extraction buffer (NEB) (0.32 M sucrose, 5 mM CaCl₂, 3 mM Mg(Ac)₂, 0.1 mM EDTA, 10 mM Tris-HCl, and 0.1% (v/v) Triton X-100) with 30 µL of freshly added protease inhibitor cocktail (PIC, Sigma-Aldrich), 3 µL of 100 mM phenylmethylsulfonyl fluoride (PMSF, Sigma-Aldrich) in isopropyl alcohol, 3 µL of 1 M dithiothreitol (DTT, Sigma-Aldrich), and 4.5 µL of ribonuclease (RNase) inhibitor (2313A, Takara Bio). The tissue was homogenized in a tissue grinder (D9063, Sigma-Aldrich). The homogenate was filtered with a 40 µm cell strainer (22-363-547, Thermo Fisher Scientific) and collected in a 15 mL centrifuge tube. The cell suspension was centrifuged at 1000 RCF for 10 min. The supernatant was discarded, and the pellet was resuspended in 0.5 mL of ice-cold NEB with 5 µL of freshly added PIC, 0.5 µL of PMSF, 0.5 µL of DTT, and 0.75 µL of RNase inhibitor. 500 µL of the sample was mixed with 750 µL of 50%(w/v) iodixanol (made by mixing 4 mL of OptiPrep™ gradient (Sigma-Aldrich) and 0.8 mL of diluent (150 mM KCl, 30 mM MgCl₂, and 120 mM Tris-HCl)). The mixture was centrifuged at 10,000 RCF for 20 min. Then, the supernatant was removed and 300 µL of 2%(w/v) normal goat serum (50062Z, Life technologies) in Dulbecco's PBS (DPBS, Life technologies) was added to resuspend the nuclei pellet. To separate NeuN+ and NeuN- fractions, 6 µL of 2 ng/µL anti-NeuN antibody conjugated with Alexa 488 (MAB377X, Millipore) in DPBS was added into the nuclei suspension. The suspension was mixed well and incubated at 4°C for 1 h on a rotator mixer (Labnet). After incubation, the sample was sorted into NeuN+ and NeuN- fractions using a BD FACSAria™ cell sorter (BD Biosciences). The sorted NeuN+ nuclei were directly used for the RNA-seq experiment. 200 µL of sorted NeuN+ nuclei suspension, containing ~26,000 nuclei, was added into 800 µL of ice-cold PBS for ChIP-seq experiment. 200 µL of 1.8 M sucrose solution, 10 µL of 1 M CaCl₂, and 3 µL of 1 M Mg(Ac)₂ were added into the mixture. The solution was mixed well and incubated on ice for 15 min. Then, the sample was centrifuged at 1800 RCF at 4°C for 15 min. The supernatant was discarded and the pellet was resuspended in 60 µL of PBS with 0.6 µL of freshly added PIC and 0.6 µL of PMSF and stored on ice until use in the ChIP-seq.

Construction of ChIP-seq libraries

Chromatin fragments were prepared using micrococcal nuclease (MNase) to digest sorted and concentrated neuronal nuclei⁵¹. 54 µL of chromatin fragments (from 10,000 nuclei, containing approximately 60 ng of DNA) was used in each ChIP assay. Chromatin immunoprecipitation was carried out using multiplexed MOWChIP assay⁵¹ with anti-H3K4me3 (39159, Active Motif) and anti-H3K27ac (39135, Active Motif) antibody. ChIP-seq libraries were prepared using Accel-NGS 2S Plus DNA Library kit (Swift Biosciences) from purified immunoprecipitated DNA. Minor modifications were made to the manufacturer's procedures as detailed below. In the amplification step, instead of adding 10 µL of low EDTA TE buffer into each reaction, we added the mixture of 7.5 µL of low EDTA TE buffer and 2.5 µL of 20X EvaGreen dye to monitor and quantify PCR amplification. The reaction was stopped when the sample's fluorescence intensity increased by 3000 relative fluorescence units (RFU). Then, 50 µL of the mixture after PCR amplification was transferred into an Eppendorf tube and mixed with 37.5 µL of SPRIselect beads. After 5-min incubation at room temperature, the beads were cleaned with 80% ethanol. In the end, the DNA library was eluted from the beads into 7 µL of low EDTA TE buffer. The libraries were sequenced by Illumina HiSeq 4000 with single-end 50-nt reads.

Construction of RNA-seq libraries

100 µL of sorted neuronal nuclei suspension from brain tissue, containing ~12,000 nuclei to generate two replicate libraries, was used for RNA extraction by using the RNeasy Mini Kit (74104, Qiagen) and RNase-Free DNase Set (79254, Qiagen), following the manufacturers' instructions. Half of the extracted mRNA (from 6,000 nuclei) in 30-µL volume was concentrated by ethanol precipitation and resuspended in 4.6 µL of RNase-free water. RNA-seq libraries were prepared using SMART-seq v4 Ultra Low Input RNA kit (Clontech) and a Nextera XT DNA Library Preparation kit (FC-131-1024, Illumina) following the protocol and the manufacturer's instructions with minor modification. ~600 pg of purified cDNA was used for Nextera XT library preparation. ChIP-seq and RNA-seq library fragment sizes were measured using high sensitivity DNA analysis kit (5067-4626, Agilent) on a TapeStation system (2200, Agilent). ChIP-seq and RNA-seq libraries were randomly pooled together. Around 15 and 11 million reads were allocated to each ChIP-seq and RNA-seq library, respectively. The concentration of each library was examined by a KAPA library quantification kit (KK4809, Kapa Biosystems), and then the quantified libraries were pooled to reach a total concentration of 10 nM. The libraries were sequenced by Illumina HiSeq 4000 with single-end 50-nt read.

ChIP-seq data processing

The bioinformatic tools used in the data analysis are summarized in Supplementary Table. 1. Sequencing reads were trimmed using Trim Galore!⁶⁰ (Babraham Institute) with default settings. Trimmed reads were aligned to the mm10 genome with Bowtie2⁶¹. Peaks were called using MACS2⁶² ($q < 0.05$). Blacklisted regions in the mm10, as defined by ENCODE⁶³, were removed to improve data quality using SAMtools⁶⁴. Mapped reads from ChIP and input samples were extended by 100bp on either side (200 bp total) using BEDtools⁶⁵ and a normalized signal was calculated. For visualization in IGV⁶⁶ (Broad Institute), the signal was calculated in 100bp windows over the entire genome and output as a bigWig⁶⁷ file. Low-quality datasets (defined as having the number of identified peaks less than 15,000, mapping rate less than 80%, or the value of the fraction of reads in peaks (FRiP) less than 10%) were discarded.

RNA-seq data processing

Sequencing reads were trimmed under default settings using Trim Galore!⁶⁰. The trimmed reads were mapped to GRCh38 genome with hisat2⁶⁸. Mapped bam files were imported into SeqMonk⁶⁹ v1.47.1 (Babraham Institute). Low-quality datasets (with percentage of reads aligned to exons < 40%) were discarded. FeatureCounts⁷⁰ was used to count reads and DEGs were determined by pairwise comparison using DESeq2⁷¹ ($FDR < 0.05$, $|\log_2 FC| > 0.5$). The threshold of $FDR < 0.05$ was used to maintain consistency with the enhancer analysis.

Differential analysis for ChIP-seq data

Peaks were called using MACS2⁶². Peaks with $q\text{-value} < 0.05$ were taken as input for DiffBind⁷² R package. We first created consensus peak sets using Diffbind for ChIP-seq data of H3K4me3 and H3K27ac separately. Using dba.peakset function in Diffbind, “majority-rules” was applied to generate consensus peak sets for all the experimental groups (i.e., a consensus peak must be present in more than half of the replicate datasets) and then the seven calculated consensus peak sets, associated with seven conditions, were combined into a master set for analysis. The raw read counts were extracted using the function of dba.count in DiffBind, and DESeq2⁷¹ R package was used to perform the differential peaks analysis based on the TMM normalized reads to identify differential peaks between MIA and control cohorts ($FDR < 0.05$). We used DESeq2’s regression framework to adjust enhancer counts for technical variation before testing for condition effects. The following covariates were regressed out: number of peaks, number of unique reads, NSC, RSC, FRiP, and sequencing depth. For H3K27ac data, we considered

H3K27ac^{high} regions without overlap to the promoter regions to be enhancer regions. Enhancer regions were annotated to genes using existing Hi-C data⁷³, or assigned to the nearest genes when no interaction was identified. We annotated H3K4me3 peaks to genes when they overlapped with promoter regions.

Differential analysis for RNA-seq data

Genes with fewer than 10 reads in over 70% of datasets were removed before differential analysis. Raw read counts for the remaining genes were used as input for DESeq2⁷¹ for differential analysis. The following covariates were regressed out: sequencing depth, batch effect, exon percentage, and number of unique reads. Genes with FDR < 0.05 and |log₂FC| > 0.5 were identified as differentially expressed genes.

Weighted gene co-expression network analysis

The WGCNA⁷⁴ package in R was used to build the co-expression network. We first discarded low-quality data when 70% of the counts are less than 5. Then the gene expression values were normalized using log₂(FPKM) (Fragments Per Kilobase per Million mapped reads) and then genes were sorted according to their median absolute deviation (MAD). Genes with MAD value over 0.3 were used as input for network construction. The normalized gene expression values were then transformed into an adjacency matrix using the function $a_{ij} = |cor(x_i, x_j)|^\beta$, where x_i and x_j were the expression data of two genes. The value of β was determined for each group using the approximate scale-free topology⁷⁵. Topological overlap was calculated by converting the adjacency matrix into a topological overlap matrix (TOM) using the blockwiseModules function in WGCNA. Gene modules were then identified based on the TOM, and the expression profile of each module was summarized by its corresponding module eigengene. The top 100 highly connected genes within each module were identified using the softConnectivity function. To improve interpretability in the module–trait relationship plots, we normalized the values such that the largest absolute values—regardless of sign—highlight gene clusters with the strongest trait associations.

Taiji pipeline

Taiji pipeline was implemented to identify transcription factors that regulate gene expression differently between two conditions by integrating multiomics data⁷⁶. Active regulatory elements were first identified via the overlap of high confidence peaks from H3K27ac with known gene

promoter regions (4kb upstream and 1kb downstream of the transcription start sites). The distal H3K27ac peaks were assigned to active promoters using the unsupervised learning method EpiTensor⁷⁷ and assigned as an enhancer-promoter interaction if one locus overlapped with the distal peak and the other locus in the pair overlapped with a known promoter. Putative TF binding motifs were curated from the CIS-BP database. Using FIMO's algorithm, TFs were identified as having binding sites within 150-bp regions centered around H3K27ac peak summits. Network topologies were thus constructed by forming directed edges between TF and its regulated genes, if the TF had a predicted binding site in the gene's promoter or linked enhancer. Regulated genes were first extracted for all key transcription factors. If the same regulated gene was present in more than 60% of the samples, it was defined as a key regulated gene.

Enrichment of various GWAS traits

The enrichment of various GWAS traits in differential enhancers and promoters was evaluated using LD score partitioned heritability (ldsc v1.0.1)⁷⁸. The regions of differential peaks were first converted from the mm10 genome to hg38. We used summary statistics derived exclusively from individuals of European ancestry for GWAS traits with European genetic backgrounds. Default parameters were applied for the LDSC algorithm.

Results

Overview of experimental design and dataset validation

Our previous observations using a cross-fostering experimental approach showed that certain phenotypes – such as enhanced behavioral responses induced by psychoactive drugs, including classical psychedelics and dissociatives – remained dysregulated in prenatally stressed mice that were raised by control surrogate mothers⁷⁹. Similar findings have been reported by other groups using poly-(I:C)-induced MIA during pregnancy, suggesting that at least some of the long-term alterations observed in the adult offspring are a consequence of prenatal environmental insults rather than maternal adaptations after pregnancy⁸⁰. However, we also recognize that maternal perturbations induced by prenatal insults can persist beyond birth, particularly during lactation, potentially altering the relationship between pups and dams^{81, 82}. Based on these findings, we examined whether MIA-induced perturbations impact offspring's frontal cortex epigenomic and transcriptomic profiles later in life. We generated four experimental groups by administering intranasal (i.n.) infection of influenza A/WSN/33 (H1N1) virus, or mock PBS, on embryonic day 9.5 (E9.5). On the day of birth (P1), approximately half of the offspring from each group was cross-fostered. Frontal cortex tissue samples were collected in adulthood (ten-week-old mice) and profiled.

The four groups were as follows (Fig. 1):

Mock-Mock: Offspring born to control mother and raised by their birth mother, together with stepsiblings born to MIA-exposed mother.

MIA-Mock: Offspring born to MIA-exposed mother but raised by control surrogate mother, together with stepsiblings born to this control mother.

Mock-MIA: Offspring born to control mother but raised by MIA-exposed surrogate mother, together with stepsiblings born to this MIA mother.

MIA-MIA: Offspring born to MIA-exposed mother and raised by their birth mother, together with stepsiblings born to control mother.

We generated profiles on histone modifications H3K4me3 and H3K27ac as well as the transcriptome on neuronal (NeuN+) nuclei from frontal cortex of all groups. Each frontal cortex sample yielded approximately 60,000 NeuN+ nuclei. MOWChIP-seq^{50, 51} (~10,000 nuclei per library) and SMART-seq2 (~6,000 per library) were conducted with two technical replicates for each modality (H3K4me3, H3K27ac or transcriptome) of each frontal cortex sample. Our ChIP-seq datasets presented very low background with the fraction of reads in peaks (FRIP)

averaging at 22.2% and 38.8% for H3K27ac and H3K4me3 data, respectively (Supplementary Data 1). Using Phantompeakqualtools, we also calculated the normalized strand cross-correlation (NSC) and relative strand cross-correlation (RSC) to demonstrate enrichment of sequencing reads around the histone modification sites. The average NSCs were 1.14 and 1.3 for H3K27ac and H3K4me3, respectively; and the average RSCs were 4.57 and 1.85, respectively. These values compare favorably with the ENCODE recommended thresholds of 1.05 and 1.0 for NSC and RSC, respectively. Our RNA-seq datasets had an average mapping rate of 93.49%, higher than the recommended range of 80-90%⁸³ (Supplementary Data 1). Each RNA-seq dataset covered an average of 18,667 genes. Our average GC content was 41.7% and the average exon percentage was 62.7%.

We conducted overlap analysis to generate consensus peak sets for neuronal H3K27ac and H3K4me3 by collecting consensus peaks that were called in at least half of the datasets in a condition. We identified 49,537 consensus peaks covering ~162 Mb (5.95% of the genome) for H3K27ac and 64,512 consensus peaks covering ~164 Mb (6.02% of the genome) for H3K4me3. Cis-regulatory elements such as promoters and enhancers are non-coding DNA elements that regulate gene activities⁸⁴. Delineation of promoters and enhancers is essential for understanding the alterations in gene regulation patterns associated with neuronal development, synaptic formation, and dendritic growth^{58, 59, 85}. We identified active promoters and enhancers by scanning H3K4me3^{high} regions that intersected with promoters and H3K27ac^{high} regions that did not have any overlap with promoters⁸⁶, respectively. We generated 36,480 (covering ~115 Mb) and 18,008 (covering ~68 Mb) putative active enhancers and promoters in neurons, respectively.

The PCA analyses of promoter, enhancer, and RNA-seq datasets consistently showed that samples grouped according to their prenatal and postnatal treatment conditions (Supplementary Fig.1—3). Enhancer-based PCA showed greater positional differences between groups than promoter-based PCA, reflecting the relative stability of promoter-associated H3K4me3 compared to the variability of enhancer-associated H3K27ac. Consistent with this, differentially expressed genes showed weak overlap with differentially H3K4me3-enriched promoters and were substantially more abundant, indicating that many transcriptional alterations arise from distal enhancer activity and other regulatory mechanisms rather than promoter remodeling.

Epigenomic and transcriptomic alterations caused by prenatal effects of MIA

We employed cross-fostering to separate the prenatal and postnatal effects of MIA on offspring (Fig. 1). Mock-Mock and MIA-Mock groups share the same postnatal fostering condition but differ in the prenatal impact of MIA. The situation is similar when Mock-MIA and MIA-MIA are compared. We regressed out confounding covariates including FRIP, the number of unique reads, and sequencing depth. We identified 3350 differential enhancers, 495 differential promoters, and 2638 differentially expressed genes (DEGs) between Mock-Mock and MIA-Mock with a false discovery rate (FDR) of less than 0.05 and $|\log_2\text{FC}| > 0.5$. When Mock-MIA and MIA-MIA are compared, we identified 5072 differential enhancers, 149 differential promoters and 2398 DEGs (Fig. 2a). We linked differential enhancers to genes based on Hi-C data⁷³ first, then to their nearest genes. Differential promoters are linked to their nearest genes.

The DEGs between Mock-Mock and MIA-Mock include *Adam22*($-\log_{10}(\text{FDR})=17.64$), *Ogt*($-\log_{10}(\text{FDR})=14.87$), and *Nfrkb*($-\log_{10}(\text{FDR})=14.40$) (Supplementary Fig. 4a and Supplementary Data 2). In the second prenatal comparison (Mock-MIA vs. MIA-MIA), DEGs included *Igsf9b*($-\log_{10}(\text{FDR})=16.70$), *Plxna4*($-\log_{10}(\text{FDR})=17.36$), and *Arhgef2*($-\log_{10}(\text{FDR})=16.43$) (Supplementary Fig. 4b).

We then identified genes showing coordinated epigenomic (i.e. enhancer or promoter) and expression differences ($|\log_2\text{FC}| > 0.5$, FDR < 0.05) (Supplementary Data 3, Fig. 2b). A total of 357 such genes were identified in the Mock-Mock vs. MIA-Mock comparison. The KEGG terms associated with these genes included glutamatergic synapse, cAMP signaling, GnRH secretion, and retrograde endocannabinoid signaling (FDR-adjusted p-value < 0.05) (Fig. 2c). In the Mock-MIA and MIA-MIA comparison, we identified 413 genes that were affected at both epigenomic and transcriptomic levels (Fig. 2b). These genes are associated with KEGG terms related to neurotransmission and neural signaling including axon guidance, cAMP signaling pathway, retrograde endocannabinoid signaling pathway, dopaminergic synapse, apelin signaling pathway, and pathways of neurodegenerative diseases (FDR < 0.05) (Fig. 2d). Many of these pathways are directly implicated in prenatal brain development and psychiatric risk. Increasing evidence suggests that glutamatergic synapses, linked to many neurotransmitter pathways, contribute to various neurodevelopmental disorders⁸⁷. cAMP signaling is closely associated with dopamine receptor activation⁸⁸, and it is linked to psychotic depression⁸⁹. GnRH neurons play an essential role in the formation and integration of the neuronal network⁹⁰. The retrograde endocannabinoid signaling pathway plays a critical role in regulating stress and anxiety⁹¹.

Malfunction of the dopamine system in the prefrontal cortex contributes to the cognitive and negative symptoms of schizophrenia^{92, 93}. Previous studies showed that apelin system is related to emotional behavior^{94, 95} and depression due to its involvement in the hypothalamic-pituitary-adrenal (HPA) axis⁹⁶. The higher level of cytokine caused by MIA can trigger the misguidance of neurons, which could also alter axon guidance processes⁹⁷.

To isolate prenatal effects on enhancers, we identified 1,720 overlapping differential enhancer peaks between the two prenatal comparisons (Mock-Mock vs. MIA-Mock and Mock-MIA vs. MIA-MIA) (Fig. 3a). We annotated them to genes (Fig. 3a) using existing HiC⁷³ data first, then the rest of the peaks with their closest genes. In addition to the KEGG terms discovered from the individual comparisons (glutamatergic synapse, retrograde endocannabinoid signaling, and dopaminergic synapse), we also found KEGG terms such as GABAergic synapse and MAPK signaling that are related to neurodevelopmental disorders. Previous studies have provided evidence of significant alterations in the developmental shift of GABA (gamma-aminobutyric acid) in the offspring's brain following MIA⁹⁸. The MAPK signaling pathway is also implicated in the frontal cortex of schizophrenia subjects⁹⁹. Interestingly, KEGG terms such as nicotine addiction and morphine addiction are also present. Studies suggest that pups exposed to maternal immune activation have higher motivation for cocaine self-administration¹⁰⁰. Taken together, MIA during the prenatal stage alters enhancer and promoter activities and induces transcriptomic changes in genes involved in neurotransmission, synaptic development, and disease risk. These findings support a model in which MIA disrupts core neurobiological processes relevant to neuropsychiatric and addiction disorders.

Finally, to examine the level of background within differential analyses, we also conducted differential analysis of two additional control groups (Supplementary Fig. 5):

Mock-Mock_1: Offspring born to control mother and raised by their birth mother, together with stepsiblings born to a different control mother.

Mock-Mock_2: Offspring born to control mother but raised by control surrogate mother, together with stepsiblings born to the control surrogate mother.

Between groups Mock-Mock_1 and Mock-Mock_2, we identified 648 differential enhancers, 156 differential promoters, and 350 differentially expressed genes (DEGs) ($FDR < 0.05$, $|\log_2FC| > 0.5$) (Supplementary Fig. 5b). These numbers of differential enhancers, promoters, and DEGs are notably lower than those obtained between groups involving prenatal effects. Although we identified autism¹⁰¹ related gene *Smc1a* ($-\log_{10}(FDR)=7.95$) among the DEGs, only 18 genes

overlapped between differential-enhancer/promoter-associated genes and DEGs (Supplementary Fig. 5c). No enriched KEGG terms were identified with these genes. Overall, the background signal in the differential analysis does not affect our conclusions.

Epigenomic and transcriptomic alterations caused by postnatal effects of MIA

To study the postnatal effects of MIA, we compared Mock-MIA with Mock-Mock and also MIA-Mock with MIA-MIA. The differences revealed by these two comparisons indicate whether fostering by a MIA mother induces epigenomic and transcriptomic alterations in offspring. We identified 5134 differential enhancers, 335 differential promoters, and 2723 DEGs between Mock-MIA and Mock-Mock ($|log_2FC| > 0.5$, FDR < 0.05) (Fig. 4a). We also identified 5174 differential enhancers, 254 differential promoters, and 1557 DEGs between MIA-Mock and MIA-MIA ($|log_2FC| > 0.5$, FDR < 0.05) (Fig. 4a). The DEGs between Mock-MIA and Mock-Mock include *Kctd16*($-\log_{10}(FDR)=20.04$), *Tecr*($-\log_{10}(FDR)=17.12$), *Igsf9b*($-\log_{10}(FDR)=17.82$), and *Tm2d3*($-\log_{10}(FDR)=15.53$) (Supplementary Fig. 4c). The significant DEGs identified between MIA-Mock and MIA-MIA include *Kidins220*¹⁰², ¹⁰³($-\log_{10}(FDR)=10.35$), *Pcdhg5*¹⁰⁴($-\log_{10}(FDR)=10.05$), and *Arfgef3*¹⁰⁵($-\log_{10}(FDR)=9.00$) (Supplementary Fig. 4d).

Next, we prioritized genes associated with both epigenomic and transcriptomic changes. We identified 477 genes in the comparison of Mock-MIA vs. Mock-Mock. We identified 299 genes in the comparison of MIA-Mock vs. MIA-MIA (Fig. 4b). The first group of 477 genes is enriched for KEGG terms related to several neurodegenerative diseases, including spinocerebellar ataxia and Alzheimer's disease. Additionally, we identified KEGG terms (FDR < 0.05) related to neurodevelopment similar to the ones associated with prenatal effects, such as glutamatergic synapse, cAMP signaling pathway, retrograde endocannabinoid signaling, and tight junction⁹⁷, ¹⁰⁶ (Fig. 4c). The second group of 299 genes enriches a number of KEGG terms that also relate to synaptic signaling, addiction-related pathways and neurodegenerative diseases including GABAergic and glutamatergic synapses, nicotine addiction, and Alzheimer's disease (Fig. 4d). These findings suggest that postnatal MIA exposure alters molecular programs involved in synaptic plasticity and neurobehavioral regulation, potentially linking immune experience during early life to long-term risk for both neurodevelopmental and neuropsychiatric conditions.

We identified 1708 overlapping differential enhancer peaks between the two comparisons (Mock-MIA vs. Mock-Mock and MIA-Mock vs. MIA-MIA). These represent enhancers that are the most related to postnatal effects of MIA. We generated enriched KEGG terms with the annotated genes from these peaks (Fig. 3b). We found enriched neurotransmission and neuromodulation pathways such as cAMP signaling pathway, GABAergic synapse, glutamatergic synapse, MAPK signaling pathway and dopaminergic synapse, and also terms related to addiction, including nicotine addiction, morphine addiction, and amphetamine addiction. The WNT pathway is recognized as a significant contributor to embryonic development and to conditions such as Alzheimer's disease and metabolic disorders¹⁰⁷. Compared to prenatal effects, postnatal effects are associated with a broader set of KEGG terms related to neurodegenerative pathways.

Finally, we examined the impact of maternal and peer separations¹⁰⁸ that are potentially involved in cross-fostering and our postnatal analysis as a background. Between groups Mock-Mock_1 and Mock-Mock_3 (offspring born to control mother and raised by their birth mother, without any cross-fostering manipulation), we identified 469 differential enhancers, 108 differential promoters, and 1693 DEGs ($|log_2FC| > 0.5$, FDR < 0.05) (Supplementary Fig. 5b, Supplementary Data 2). Between groups Mock-Mock_2 and Mock-Mock_3, we identified 348 differential enhancers, 648 differential promoters, and 1222 DEGs (Supplementary Data 2) under the same criteria. We found 45 and 57 overlapping genes between differential enhancer/promoter and DEGs for Mock-Mock_1 vs. Mock-Mock_3 and Mock-Mock_2 vs. Mock-Mock_3, respectively (Supplementary Fig. 5c). The 57 overlapping genes for Mock-Mock_2 versus Mock-Mock_3 exhibit enriched KEGG pathways including GnRH related pathway, glutamatergic synapse and cAMP signaling pathway (Supplementary Fig. 5d). We discovered *Egr2* among the DEGs for Mock-Mock_1 vs. Mock-Mock_3. *Egr2* has been linked to peripheral neuropathy phenotypes in previous studies¹⁰⁹ (Supplementary Fig. 6a). Additionally, *Prmt7* was found in the DEGs list for Mock-Mock_2 vs. Mock-Mock_3 and is associated with syndromic neurodevelopmental disorder¹¹⁰ (Supplementary Fig. 6c). Although all Mock-Mock groups were untreated controls, comparisons involving Mock-Mock3 showed over 1200 DEGs, while Mock-Mock1 vs. Mock-Mock2 differed by only approximately 350 DEGs. The background signal should only affect our differential analysis minimally.

Overlap between prenatal and postnatal effects at the epigenomic level

There is substantial overlap in genes impacted by prenatal and postnatal effects. We identified 599 differential-enhancer-linked genes shared between prenatal and postnatal effects, while 268 and 276 were unique differential-enhancer-linked genes involved in the prenatal and postnatal effects, respectively. Although KEGG enrichment analysis of the unique gene sets did not yield significant results, we performed Gene Ontology (GO) enrichment to identify distinct biological processes associated with prenatal and postnatal effects (Fig. 3c, d). The 268 prenatal-specific enhancer-linked genes were enriched for developmental terms such as telencephalon development, forebrain development, and central nervous system development (Fig. 3c). In contrast, the 276 postnatal-specific enhancer-linked genes were enriched for processes related to synaptic signaling, axonogenesis, and neuron differentiation (Fig. 3d). These findings highlight stage-specific regulatory effects of MIA on brain development.

K-means clustering of enhancer peaks

We conducted K-means clustering for enhancer peaks to group enhancer features into clusters that potentially generate biological insights^{111, 112}. Consensus H3K27ac peaks from the four tested conditions (Mock-Mock, MIA-Mock, Mock-MIA, and MIA-MIA) were grouped into four clusters based on H3K27ac peak intensity patterns (Supplementary Fig. 7). Clusters I and II highlight differences among the four groups. Mock-Mock serves as the baseline, as it was not exposed to MIA *in utero* or raised by MIA mothers. In cluster I, Mock-Mock exhibits the lowest signal, while MIA-Mock and Mock-MIA are comparable, and MIA-MIA shows the highest signal. Cluster I is enriched for pathways such as adrenergic signaling in cardiomyocytes, which is linked to neurotransmitter signaling¹¹³. Additionally, pathways such as neuroactive ligand-receptor interaction and amphetamine addiction are also enriched. The enriched transcription factor MEF2D has also been associated with MIA¹¹⁴. In cluster II, Mock-Mock exhibits the highest level, while MIA-Mock, Mock-MIA, and MIA-MIA show lower levels of signal. This suggests that the enhancer-associated genes in this cluster may be downregulated following exposure to MIA. The enriched pathways include glutamatergic synapses, adrenergic signaling in cardiomyocytes, axon guidance, and dopaminergic synapses, all of which are known to be related to neurotransmission or neurodevelopment. The enriched transcription factors FOSL1 and FOSL2 have been associated with the establishment of the maternal-fetal interface¹¹⁵.

WGCNA analysis reveals key transcriptomic changes

To identify gene co-expression patterns associated with MIA, we performed weighted gene co-expression network analysis (WGCNA) that clusters genes into modules based on expression

similarity and correlates them with experimental conditions¹¹⁶ (Supplementary Fig. 8a). We present gene co-expression modules correlated with experimental groups (Supplementary Fig. 8b). Among the significant modules, MEblack exhibited strong associations in MIA-Mock vs. Mock-Mock and MIA-MIA vs. Mock-MIA, indicating its relevance to prenatal MIA effects. KEGG enrichment analysis identified pathways involved in dopaminergic synapse, neuroactive ligand-receptor interaction, and cAMP signaling (Supplementary Fig. 8b). Gene network analysis highlighted *Penk*¹¹⁷ and *Tac1*¹¹⁸, associated with neuropeptide signaling (Supplementary Fig. 8c). Although MEturquoise and MEpink also demonstrated statistical significance, their biological relevance is less clear. MEturquoise exhibits positive module-trait correlations in MIA-Mock and Mock-MIA but negative correlations in Mock-Mock and MIA-MIA, suggesting complex postnatal influences. Despite its enrichment in neurodegenerative pathways, the implication of MEturquoise in prenatal MIA effects remains unclear. Similarly, MEpink, while statistically significant, lacks enriched KEGG terms, limiting its functional interpretation.

Key transcriptional regulations and regulated genes in MIA offspring

We integrated transcriptomic data with H3K27ac data to identify key transcription factors (Fig. 5) and their regulated genes using the Taiji pipeline^{76, 119}. Taiji combines diverse genomic modalities to construct transcriptional regulatory networks and predict regulatory interactions between transcription factors (TFs) and genes, using the personalized PageRank algorithm. To assess prenatal MIA effects, we compared Mock-Mock and MIA-Mock groups (Fig. 5a) and identified key transcription factors including SOX, RELA, BCL6, and EGR2. The SOX transcription factor family plays a crucial role in the development of the central nervous system. Specifically, SOX5 is identified as one of the four key regulators that primarily regulate dysregulated genes in schizophrenia within neurons. SOX5 is genetically associated with both schizophrenia and neurodevelopmental disorders (NDD), and serves as a crucial neurodevelopmental regulatory factor¹²⁰. The human gene corresponding to the transcription factor RELA is related to the development of schizophrenia¹²¹. BCL6 has been linked to Alzheimer's disease¹²². EGR2 transcription factor has been found to be linked to schizophrenia and bipolar disorder¹²³. Some of these findings on prenatal effects (i.e. RELA, BCL6, and EGR2) are also confirmed by comparing Mock-MIA and MIA-MIA (Fig. 5b). Additionally, we identified RREB1, a transcription factor essential for neuronal survival in the mammalian brain¹²⁴ and POU6F2, which regulates myelination and neurogenesis and is linked to bipolar disorder through DNA methylation¹²⁵. We also analyzed the transcription factor involvement in the postnatal effects of MIA. In the comparison of Mock-MIA vs. Mock-Mock, key transcription

factors identified include TCF3, SOX3, POU6F2 and BCL6 (Fig. 5c). The methylation pattern observed at the *Tcf3* gene is associated with T-cell maturation within the blood of schizophrenia patients¹²⁶. With MIA-Mock vs. MIA-MIA (Fig. 5d), we identified SOX5, POU6F2, RREB1 and EGR2 which were mentioned above.

Several TFs, including SOX5, BCL6, EGR2, RHOX11 and PRRX2, were consistently identified across both prenatal and postnatal comparisons. Across all comparisons, KEGG terms included cAMP signaling, axon guidance, MAPK signaling, glutamatergic synapse, and addiction-related pathways such as morphine and nicotine addiction (Fig. 5). These pathways reflect common involvement in neurotransmission, intracellular signaling and behavior regulation. Altogether, these findings indicate a conserved regulatory core associated with MIA exposure. To distinguish MIA-specific effects from baseline variation, we analyzed transcriptional regulators captured by comparisons of several control groups that do not involve MIA mothers (Supplementary Fig. 9). While TFs such as PRRX2, TCF3, and KLF family members are active, overlap with MIA-associated TFs is limited and key regulators like SOX5 and EGR2 are absent. KEGG enrichment of regulated genes (Supplementary Fig. 9) reveals broader and less consistent patterns compared to the ones involving MIA treatment. This confirms that the regulatory changes involving MIA treatment are distinct from stochastic variations.

MIA effects association with neuropsychiatric disorders

The genome-wide association studies (GWAS) employ statistical methods to establish links between genotypes and phenotypes. This is achieved by examining various genetic variants among individuals with similar genetic backgrounds but different phenotypes¹²⁷. Recent estimates suggested that over 90% of GWAS regions discovered so far are not in gene bodies but potentially on regulatory elements including promoters and enhancers¹²⁸. A total of 115 GWAS datasets focused on neurodevelopmental and neurodegenerative diseases have become available since 2007¹²⁹. A previous study confirmed the linkage between maternal immune activation and neuropsychiatric diseases such as schizophrenia and autism spectrum disorder^{130, 131}. Thus, we examined the potential association between differential enhancers and promoters discovered in this study and the human disease traits discovered by GWAS. We first utilized the genome annotation tool UCSC LiftOver to convert the differential enhancer and promoter regions from the mouse genome mm10 to the human genome hg38. The UCSC LiftOver tool has been used in many previous studies for cross-species mapping of enhancer and promoter regions^{132, 133}. Since our focus is on evolutionarily conserved regulatory regions,

UCSC LiftOver is a reliable tool. By utilizing summary statistics from GWAS with LD score regression¹³¹, we then evaluated the overlap between differential enhancers and promoters discovered in our study and GWAS regions associated with specific traits (Fig. 6). We evaluated both differential enhancers (Fig. 6a) and differential promoters (Fig. 6b) among various experimental groups. We computed the enrichment associated with schizophrenia, other neuropsychiatric disorders, and other non-psychiatric-related diseases using linkage disequilibrium (LD) score regression¹³⁴⁻¹⁴⁰.

Differential enhancer regions generally exhibit higher enrichment (-log(P) value) compared to the differential promoter regions (Fig. 6b). This suggests that the regulatory elements within enhancers may play a more prominent role in the genetic susceptibility to psychiatric disorders compared to promoters. When compared to control traits such as ulcerative colitis, type 2 diabetes, epilepsy, and celiac disease, neuropsychiatric disease traits including schizophrenia, bipolar disorder, depression, neuroticism, and ADHD show notably higher enrichment. In both prenatal and postnatal comparison groups, the enrichment for psychiatric disorders including schizophrenia, bipolar disorder, depression, and neuroticism exhibits -log(P) values significantly above the threshold of P<0.05. The high -log(P) values observed for psychiatric diseases indicate a stronger genetic association with differential epigenomic features, highlighting the important contributions of both prenatal and postnatal MIA exposure to psychiatric disorders.

Discussion

Our findings reveal that MIA during pregnancy induces widespread and persistent epigenomic and transcriptomic alterations in the frontal cortex of adult offspring, with distinct contributions from both prenatal and postnatal factors. By using a cross-fostering design, we disentangled the prenatal and postnatal origins of these changes and demonstrated that MIA exerts long-lasting regulatory effects on genes and pathways involved in neurotransmission, neurodevelopment, and psychiatric disease risk. Notably, enhancer and promoter modifications, as well as DEGs, were enriched in synaptic signaling pathways – particularly those involving glutamatergic, GABAergic, and dopaminergic transmission – highlighting core molecular mechanisms potentially disrupted in disorders such as schizophrenia, autism, and depression. These data provide compelling evidence that MIA not only reprograms early developmental trajectories through epigenetic mechanisms but also leaves a molecular footprint that may underlie behavioral phenotypes and increased vulnerability to neuropsychiatric and neurodegenerative diseases later in life.

The relative contributions of prenatal and postnatal environments to brain development remain an area of active investigation. Studies suggest that prenatal exposures exert long-term effects through hormonal signaling, immune activation, and epigenetic reprogramming during critical gestational windows^{141, 142}, whereas postnatal experiences are thought to shape synaptic refinement and circuit-level plasticity through sensory input and maternal care^{143, 144}. In influenza-based MIA models, maternal immune activation leads to elevated cytokine production, including IL-6, IL-8, IL-10, IL-17a, IFN- α , and TNF- α , which can alter placental signaling, disrupt fetal neurogenesis, and impact long-term cortical structure and behavior¹⁴⁵⁻¹⁵². Postnatal effects may result from persistent maternal immune dysregulation affecting lactation or maternal care^{153, 154}. However, the biological continuity between these periods complicates interpretation, and direct comparisons are often confounded by shared maternal or environmental effects¹⁵⁵. By applying the cross-fostering design, our model reduces these confounds, enabling clearer attribution of observed effects to the timing of maternal immune challenge. It is worth noting that the presence of cross-fostered groups within the same cage potentially leads to some level of microbiota homogenization¹⁵⁶ that may affect the observed transcriptional and epigenetic changes due to MIA.

Our results highlighted significant genes across comparison groups. For prenatal comparison, we discovered DEGs including *Adam22*($-\log_{10}(\text{FDR})=17.64$), *Ogt*($-\log_{10}(\text{FDR})=14.87$), *Nfrkb*($-\log_{10}(\text{FDR})=14.40$), *Igsf9b*($-\log_{10}(\text{FDR})=16.70$), *Plxna4*($-\log_{10}(\text{FDR})=17.36$), and *Arhgef2*($-\log_{10}(\text{FDR})=16.43$). The *Adam* family, especially *Adam22*, plays an important role in peripheral myelination¹⁵⁷. *Ogt* is involved in the embryonic development and the regulation of gene expression within the nervous system¹⁵⁸. *Nfrkb* or *NF- κ B* is a central regulator of inflammation and immune response¹⁵⁹. Variants in *Igsf9b* are associated with schizophrenia and bipolar disorder¹⁶⁰. The *Plxna4* gene has been linked to Alzheimer disease in humans through GWAS study¹⁶¹. *Arhgef2* mutations have been implicated in neurodevelopmental disorders¹⁶². For postnatal comparison, we discovered DEGs including *Kctd16*($-\log_{10}(\text{FDR})=20.04$), *Tecr*($-\log_{10}(\text{FDR})=17.12$), *Igsf9b*($-\log_{10}(\text{FDR})=17.82$), and *Tm2d3*($-\log_{10}(\text{FDR})=15.53$). The upregulation of *Kctd16* is consistent with previous findings from MIA studies¹⁶³. *Tm2d3* has been linked to late-onset Alzheimer's disease (AD) through an exome-wide association study¹⁶⁴. We also identified *Kidins220*^{102, 103}($-\log_{10}(\text{FDR})=10.35$), *Pcdhg5*¹⁰⁴($-\log_{10}(\text{FDR})=10.05$),

and *Arfgef3*¹⁰⁵ ($-\log_{10}(\text{FDR})=9.00$), from postnatal comparison, all of which are associated with schizophrenia and potentially other neurodevelopmental disorders.

Our results suggest that the prenatal and postnatal effects of MIA have substantial overlap in terms of the genes being affected at the epigenomic level. We identified 599 enhancer-associated genes shared between prenatal and postnatal changes, representing a substantial fraction of each group (867 for prenatal, 875 for postnatal). These shared genes were enriched in synaptic signaling pathways related to glutamatergic, dopaminergic, and GABAergic transmission. The overlap between prenatal and postnatal effects suggests the persistence of a core regulatory program across different developmental stages. On the other hand, prenatal-specific enhancers are enriched for gene ontology terms related to forebrain and telencephalon development, while postnatal-specific enhancers are linked to axonogenesis and synapse organization. These patterns reflect distinct neurodevelopmental programs, with prenatal regulation driving early brain patterning and progenitor expansion, and postnatal regulation supporting synaptic refinement and network integration^{165, 166}. This stage specificity may arise from dynamic shifts in enhancer activity aligned with developmental priorities.

Transcription factor (TF) motif analysis further supported this view. TFs such as SOX5, BCL6, EGR2, RHOX11, and PRRX2 were active across both developmental stages. Previous studies indicate that some of these TFs, including SOX5, BCL6 and EGR2 are altered in frontal cortex samples from both schizophrenia subjects and adult MIA mice^{21, 120, 122, 123}. The recurrence of these key neurodevelopmental TFs aligns with the shared enhancer–gene associations, indicating a common upstream regulatory architecture.

To evaluate the relevance of these regulatory elements to human disease, we performed cross-species LD score regression, mapping mouse differential enhancer/promoter regions to the human genome and integrating GWAS summary statistics. We observed strong enrichment of prenatal enhancer regions for neuropsychiatric traits, including schizophrenia, bipolar disorder, and depression. Postnatal-related differential enhancer regions exhibited similarly high enrichment. While LD score enrichment does not establish causality, it provides evidence that MIA-related regulatory elements overlap with genetic risk loci for neuropsychiatric diseases.

Our analysis also revealed enrichment of addiction-related pathways in both prenatal and postnatal effects of MIA, including those involved in morphine and nicotine addiction, suggesting

that MIA may alter regulatory programs linked to substance use vulnerability. Previous studies have reported conflicting behavioral outcomes. For example, a study of prenatal LPS exposure showed no effect on cocaine self-administration¹⁶⁷, suggesting that MIA alone may not enhance vulnerability to addiction. In contrast, another study demonstrated that while MIA increased the likelihood of acquiring cocaine self-administration, it did not influence the amount of cocaine intake once the behavior was established¹⁰⁰. Moreover, when combined with adolescent alcohol exposure, MIA has been shown to increase alcohol intake and disrupt corticostriatal oscillations¹⁶⁸. These findings suggest that MIA may not directly induce addictive behaviors, but instead prime neural circuits involved in reward and reinforcement, thereby increasing sensitivity to later environmental challenges.

Beyond pathways associated with reward processing, we also observed enrichment of broader GO categories such as brain development, nervous system development, and synaptic signaling, indicating that MIA impacts fundamental neurodevelopmental and synaptic organization processes. The transcriptional and epigenetic alterations identified in glutamatergic, GABAergic, and dopaminergic systems could directly affect neuronal excitability and circuit function, though the extent to which these molecular changes translate into behavioral outcomes remains unknown. Alternatively, they may reflect a primed state that increases vulnerability to subsequent stressors or environmental exposures^{144, 169}. Previous evidence suggests that maternal immune activation can reconfigure neuroimmune and synaptic systems, creating long-lasting sensitivity that remains latent until later challenges emerge^{7, 170-172}.

Early-life stress (ELS) and maternal immune activation share several convergent biological themes including the effects on hypothalamic–pituitary–adrenal (HPA) axis pathways and dopaminergic circuits^{152, 173-175}. Studies also show ELS related pathways including impaired cellular maintenance, metabolic dysfunction, and long-lasting glial or neuronal alterations¹⁷⁶⁻¹⁷⁸. We did not observe direct enrichment of HPA axis pathways, which are frequently implicated in ELS models^{173, 179}, although we detected effects of MIA on neuronal alterations and dopaminergic circuits.

In addition to these neuronal regulatory mechanisms, non-neuronal cells also play a central role in mediating and amplifying immune-driven effects on brain development¹⁸⁰. Although this study focused on NeuN⁺ neuronal nuclei to capture gene regulatory changes linked to neuronal

function, glial populations constitute an equally important component of the brain's response to immune challenge. Microglia and astrocytes regulate synaptic development, cytokine signaling, and stress reactivity, and their dysfunction has been implicated in MIA-related and psychiatric phenotypes^{7, 181, 182}. Integrating glial-specific transcriptomic and epigenomic profiling in future work will be critical for resolving the full cellular spectrum of MIA-induced alterations.

Maternal immune activation can lead to diverse outcomes among exposed offspring. Some develop strong behavioral or molecular alterations, while others remain unaffected or show adaptive responses^{7, 172}. This variation likely reflects differences in genetic background, immune activation strength and timing, and postnatal conditions¹⁷². Maternal factors also shape offspring response: adequate micronutrient levels (vitamin D, iron, zinc), balanced omega-3 fatty acids, and effective antioxidant or anti-inflammatory systems promote resilience, whereas hypoferremia, gestational diabetes, stress, and microbiome imbalance increase risk^{7, 172}. Our study did not assess maternal health or nutrition, but these variables may influence offspring outcomes and should be considered in future work. Although resilience after MIA has been reported, studies directly examining resilience to depression-like effects are limited. Insights from depression and stress research suggest that stable HPA-axis control, efficient immune resolution, intact synaptic plasticity, and supportive environments can buffer against depressive outcomes^{179, 183, 184}. Future studies should explore these protective mechanisms within MIA models.

Taken together, our study underscores the enduring impact of MIA on the epigenomic landscape of the developing brain, with both prenatal and postnatal stages contributing to long-term regulatory alterations in pathways critical for neuropsychiatric disease risk. By integrating transcriptomic, epigenomic, and cross-species analyses, we provide mechanistic insights into how early-life immune challenges shape brain function and vulnerability to psychiatric and substance use disorders. Our work defines the epigenomic framework linking MIA to altered gene regulation and highlights biological pathways for future mechanistic investigation. Finally, these findings highlight the importance of temporal context in neurodevelopmental risk, suggesting that interventions aimed at mitigating the effects of MIA may need to consider both gestational and early postnatal windows.

Data availability

RNA-seq and ChIP-seq data discussed in this publication have been deposited in NCBI's Gene Expression Omnibus and are accessible through GEO Series accession numbers GSE297245 (<https://www.ncbi.nlm.nih.gov/geo/query/acc.cgi?acc=GSE297245>) and GSE297247 (<https://www.ncbi.nlm.nih.gov/geo/query/acc.cgi?acc=GSE297247>), respectively. All processed data and Supplementary Information are provided with the paper. Additional information and materials are available from the corresponding author upon reasonable request.

Code availability

All code is available at GitHub (https://github.com/changlulab/zhu_Li_et_al_2025).

Ethics approval and consent to participate

Experiments were conducted in accordance with NIH guidelines and were approved by the Virginia Commonwealth University Animal Care and Use Committee under the reference number AD10001212.

References

1. Stiles J, Jernigan TL. The basics of brain development. *Neuropsychol Rev* 2010; 20(4): 327-348.
2. Garay PA, McAllister AK. Novel roles for immune molecules in neural development: implications for neurodevelopmental disorders. *Front Synaptic Neurosci* 2010; 2: 136.
3. Bergdolt L, Dunaevsky A. Brain changes in a maternal immune activation model of neurodevelopmental brain disorders. *Prog Neurobiol* 2019; 175: 1-19.
4. Bale TL. Epigenetic and transgenerational reprogramming of brain development. *Nat Rev Neurosci* 2015; 16(6): 332-344.
5. Solek CM, Farooqi N, Verly M, Lim TK, Ruthazer ES. Maternal immune activation in neurodevelopmental disorders. *Dev Dyn* 2018; 247(4): 588-619.
6. Instanes JT, Halmoy A, Engeland A, Haavik J, Furu K, Klungsoyr K. Attention-Deficit/Hyperactivity Disorder in Offspring of Mothers With Inflammatory and Immune System Diseases. *Biol Psychiatry* 2017; 81(5): 452-459.
7. Estes ML, McAllister AK. Maternal immune activation: Implications for neuropsychiatric disorders. *Science* 2016; 353(6301): 772-777.
8. Careaga M, Murai T, Bauman MD. Maternal Immune Activation and Autism Spectrum Disorder: From Rodents to Nonhuman and Human Primates. *Biol Psychiatry* 2017; 81(5): 391-401.
9. Canetta SE, Brown AS. Prenatal Infection, Maternal Immune Activation, and Risk for Schizophrenia. *Transl Neurosci* 2012; 3(4): 320-327.
10. Brown AS, Meyer U. Maternal Immune Activation and Neuropsychiatric Illness: A Translational Research Perspective. *Am J Psychiatry* 2018; 175(11): 1073-1083.
11. Knuesel I, Chicha L, Britschgi M, Schobel SA, Bodmer M, Hellings JA et al. Maternal immune activation and abnormal brain development across CNS disorders. *Nat Rev Neurol* 2014; 10(11): 643-660.
12. Brown AS, Begg MD, Gravenstein S, Schaefer CA, Wyatt RJ, Bresnahan M et al. Serologic evidence of prenatal influenza in the etiology of schizophrenia. *Arch Gen Psychiatry* 2004; 61(8): 774-780.
13. Susser ES, Schaefer CA, Brown AS, Begg MD, Wyatt RJ. The design of the prenatal determinants of schizophrenia study. *Schizophr Bull* 2000; 26(2): 257-273.

14. Fortier ME, Luheshi GN, Boksa P. Effects of prenatal infection on prepulse inhibition in the rat depend on the nature of the infectious agent and the stage of pregnancy. *Behav Brain Res* 2007; 181(2): 270-277.
15. Fortier ME, Joober R, Luheshi GN, Boksa P. Maternal exposure to bacterial endotoxin during pregnancy enhances amphetamine-induced locomotion and startle responses in adult rat offspring. *J Psychiatr Res* 2004; 38(3): 335-345.
16. Coyle P, Tran N, Fung JN, Summers BL, Rofe AM. Maternal dietary zinc supplementation prevents aberrant behaviour in an object recognition task in mice offspring exposed to LPS in early pregnancy. *Behav Brain Res* 2009; 197(1): 210-218.
17. Krstic D, Madhusudan A, Doechner J, Vogel P, Notter T, Imhof C et al. Systemic immune challenges trigger and drive Alzheimer-like neuropathology in mice. *J Neuroinflammation* 2012; 9: 151.
18. Giovanoli S, Engler H, Engler A, Richetto J, Voget M, Willi R et al. Stress in puberty unmasks latent neuropathological consequences of prenatal immune activation in mice. *Science* 2013; 339(6123): 1095-1099.
19. Deverman BE, Patterson PH. Cytokines and CNS Development. *Neuron* 2009; 64(1): 61-78.
20. Holloway T, González-Maeso J. Epigenetic Mechanisms of Serotonin Signaling. *ACS Chem Neurosci* 2015; 6(7): 1099-1109.
21. Moreno JL, Kurita M, Holloway T, López J, Cadagan R, Martínez-Sobrido L et al. Maternal influenza viral infection causes schizophrenia-like alterations of 5-HT_{2A} and mGlu₂ receptors in the adult offspring. *J Neurosci* 2011; 31(5): 1863-1872.
22. Saunders JM, Moreno JL, Ibi D, Sikaroodi M, Kang DJ, Muñoz-Moreno R et al. Gut microbiota manipulation during the prepubertal period shapes behavioral abnormalities in a mouse neurodevelopmental disorder model. *Sci Rep* 2020; 10(1): 4697.
23. Saunders JM, Muguruza C, Sierra S, Moreno JL, Callado LF, Meana JJ et al. Glucocorticoid receptor dysregulation underlies 5-HT(2A)R-dependent synaptic and behavioral deficits in a mouse neurodevelopmental disorder model. *J Biol Chem* 2022; 298(11): 102481.
24. Kolk SM, Rakic P. Development of prefrontal cortex. *Neuropsychopharmacology* 2022; 47(1): 41-57.
25. Andersen SL. Trajectories of brain development: point of vulnerability or window of opportunity? *Neurosci Biobehav Rev* 2003; 27(1-2): 3-18.

26. Friedman NP, Robbins TW. The role of prefrontal cortex in cognitive control and executive function. *Neuropsychopharmacology* 2022; 47(1): 72-89.
27. Rubenstein JL, Merzenich MM. Model of autism: increased ratio of excitation/inhibition in key neural systems. *Genes Brain Behav* 2003; 2(5): 255-267.
28. Shrestha S, Offer SM. Epigenetic Regulations of GABAergic Neurotransmission: Relevance for Neurological Disorders and Epigenetic Therapy. *Medical Epigenetics* 2016; 4(1): 1-19.
29. Stadler F, Kolb G, Rubusch L, Baker SP, Jones EG, Akbarian S. Histone methylation at gene promoters is associated with developmental regulation and region-specific expression of ionotropic and metabotropic glutamate receptors in human brain. *J Neurochem* 2005; 94(2): 324-336.
30. Sun E, Shi Y. MicroRNAs: Small molecules with big roles in neurodevelopment and diseases. *Exp Neurol* 2015; 268: 46-53.
31. Richetto J, Meyer U. Epigenetic Modifications in Schizophrenia and Related Disorders: Molecular Scars of Environmental Exposures and Source of Phenotypic Variability. *Biol Psychiatry* 2021; 89(3): 215-226.
32. Labouesse MA, Dong E, Grayson DR, Guidotti A, Meyer U. Maternal immune activation induces GAD1 and GAD2 promoter remodeling in the offspring prefrontal cortex. *Epigenetics* 2015; 10(12): 1143-1155.
33. Ma L, Wang F, Li Y, Wang J, Chang Q, Du Y et al. Brain methylome remodeling selectively regulates neuronal activity genes linking to emotional behaviors in mice exposed to maternal immune activation. *Nature Communications* 2023; 14(1): 7829.
34. Tang B, Jia H, Kast RJ, Thomas EA. Epigenetic changes at gene promoters in response to immune activation in utero. *Brain Behav Immun* 2013; 30: 168-175.
35. Reisinger SN, Kong E, Khan D, Schulz S, Ronovsky M, Berger S et al. Maternal immune activation epigenetically regulates hippocampal serotonin transporter levels. *Neurobiol Stress* 2016; 4: 34-43.
36. Won H, Huang J, Opland CK, Hartl CL, Geschwind DH. Human evolved regulatory elements modulate genes involved in cortical expansion and neurodevelopmental disease susceptibility. *Nat Commun* 2019; 10(1): 2396.

37. Dincer A, Gavin DP, Xu K, Zhang B, Dudley JT, Schadt EE *et al.* Deciphering H3K4me3 broad domains associated with gene-regulatory networks and conserved epigenomic landscapes in the human brain. *Transl Psychiatry* 2015; 5: e679.
38. Kim M, Costello J. DNA methylation: an epigenetic mark of cellular memory. *Experimental & Molecular Medicine* 2017; 49(4): e322-e322.
39. Bannister AJ, Kouzarides T. Regulation of chromatin by histone modifications. *Cell Research* 2011; 21(3): 381-395.
40. Connor CM, Dincer A, Straubhaar J, Galler JR, Houston IB, Akbarian S. Maternal immune activation alters behavior in adult offspring, with subtle changes in the cortical transcriptome and epigenome. *Schizophr Res* 2012; 140(1-3): 175-184.
41. Meyer U. Prenatal poly(i:C) exposure and other developmental immune activation models in rodent systems. *Biol Psychiatry* 2014; 75(4): 307-315.
42. Harvey L, Boksa P. Prenatal and postnatal animal models of immune activation: relevance to a range of neurodevelopmental disorders. *Dev Neurobiol* 2012; 72(10): 1335-1348.
43. Kentner AC, Bilbo SD, Brown AS, Hsiao EY, McAllister AK, Meyer U *et al.* Maternal immune activation: reporting guidelines to improve the rigor, reproducibility, and transparency of the model. *Neuropsychopharmacology* 2019; 44(2): 245-258.
44. Bauman MD, Iosif AM, Smith SE, Bregere C, Amaral DG, Patterson PH. Activation of the maternal immune system during pregnancy alters behavioral development of rhesus monkey offspring. *Biol Psychiatry* 2014; 75(4): 332-341.
45. Machado CJ, Whitaker AM, Smith SE, Patterson PH, Bauman MD. Maternal immune activation in nonhuman primates alters social attention in juvenile offspring. *Biol Psychiatry* 2015; 77(9): 823-832.
46. Reisinger S, Khan D, Kong E, Berger A, Pollak A, Pollak DD. The poly(I:C)-induced maternal immune activation model in preclinical neuropsychiatric drug discovery. *Pharmacol Ther* 2015; 149: 213-226.
47. Weber-Stadlbauer U, Richetto J, Zwamborn RAJ, Slieker RC, Meyer U. Transgenerational modification of dopaminergic dysfunctions induced by maternal immune activation. *Neuropsychopharmacology* 2021; 46(2): 404-412.
48. Lin YL, Lin SY, Wang S. Prenatal lipopolysaccharide exposure increases anxiety-like behaviors and enhances stress-induced corticosterone responses in adult rats. *Brain Behav Immun* 2012; 26(3): 459-468.

49. Aoshi T, Koyama S, Kobiyama K, Akira S, Ishii KJ. Innate and adaptive immune responses to viral infection and vaccination. *Curr Opin Virol* 2011; 1(4): 226-232.
50. Cao Z, Chen C, He B, Tan K, Lu C. A microfluidic device for epigenomic profiling using 100 cells. *Nat Methods* 2015; 12(10): 959-962.
51. Zhu B, Hsieh YP, Murphy TW, Zhang Q, Naler LB, Lu C. MOWChIP-seq for low-input and multiplexed profiling of genome-wide histone modifications. *Nat Protoc* 2019; 14(12): 3366-3394.
52. Liu Z, Naler LB, Zhu Y, Deng C, Zhang Q, Zhu B et al. nMOWChIP-seq: low-input genome-wide mapping of non-histone targets. *NAR Genom Bioinform* 2022; 4(2): lqac030.
53. Picelli S, Faridani OR, Bjorklund AK, Winberg G, Sagasser S, Sandberg R. Full-length RNA-seq from single cells using Smart-seq2. *Nat Protoc* 2014; 9(1): 171-181.
54. Picelli S, Bjorklund AK, Faridani OR, Sagasser S, Winberg G, Sandberg R. Smart-seq2 for sensitive full-length transcriptome profiling in single cells. *Nat Methods* 2013; 10(11): 1096-1098.
55. Kellendonk C, Simpson EH, Kandel ER. Modeling cognitive endophenotypes of schizophrenia in mice. *Trends Neurosci* 2009; 32(6): 347-358.
56. Clancy B, Finlay BL, Darlington RB, Anand KJ. Extrapolating brain development from experimental species to humans. *Neurotoxicology* 2007; 28(5): 931-937.
57. Brown AS, Derkets EJ. Prenatal infection and schizophrenia: a review of epidemiologic and translational studies. *Am J Psychiatry* 2010; 167(3): 261-280.
58. de la Fuente Revenga M, Zhu B, Guevara CA, Naler LB, Saunders JM, Zhou Z et al. Prolonged epigenomic and synaptic plasticity alterations following single exposure to a psychedelic in mice. *Cell Rep* 2021; 37(3): 109836.
59. Zhu B, Ainsworth RI, Wang Z, Liu Z, Sierra S, Deng C et al. Antipsychotic-induced epigenomic reorganization in frontal cortex of individuals with schizophrenia. *Elife* 2024; 12.
60. Martin M. Cutadapt removes adapter sequences from high-throughput sequencing reads. *2011* 2011; 17(1): 3.
61. Langmead B, Salzberg SL. Fast gapped-read alignment with Bowtie 2. *Nat Methods* 2012; 9(4): 357-359.

62. Gaspar JM. Improved peak-calling with MACS2. *bioRxiv* 2018; 496521.
63. An integrated encyclopedia of DNA elements in the human genome. *Nature* 2012; 489(7414): 57-74.
64. Danecek P, Bonfield JK, Liddle J, Marshall J, Ohan V, Pollard MO *et al.* Twelve years of SAMtools and BCFtools. *Gigascience* 2021; 10(2).
65. Quinlan AR, Hall IM. BEDTools: a flexible suite of utilities for comparing genomic features. *Bioinformatics* 2010; 26(6): 841-842.
66. Robinson JT, Thorvaldsdóttir H, Winckler W, Guttman M, Lander ES, Getz G *et al.* Integrative genomics viewer. *Nat Biotechnol* 2011; 29(1): 24-26.
67. Kent WJ, Zweig AS, Barber G, Hinrichs AS, Karolchik D. BigWig and BigBed: enabling browsing of large distributed datasets. *Bioinformatics* 2010; 26(17): 2204-2207.
68. Kim D, Paggi JM, Park C, Bennett C, Salzberg SL. Graph-based genome alignment and genotyping with HISAT2 and HISAT-genotype. *Nature Biotechnology* 2019; 37(8): 907-915.
69. Babraham Bioinformatics. SeqMonk: Mapped Sequence Analysis Tool. Version 1.47.1 edn. Babraham Institute: Cambridge, UK.
70. Liao Y, Smyth GK, Shi W. featureCounts: an efficient general purpose program for assigning sequence reads to genomic features. *Bioinformatics* 2013; 30(7): 923-930.
71. Love MI, Huber W, Anders S. Moderated estimation of fold change and dispersion for RNA-seq data with DESeq2. *Genome Biology* 2014; 15(12): 550.
72. DiffBind : Differential binding analysis of ChIP-Seq peak data. 2012.
73. Bonev B, Mendelson Cohen N, Szabo Q, Fritsch L, Papadopoulos GL, Lubling Y *et al.* Multiscale 3D Genome Rewiring during Mouse Neural Development. *Cell* 2017; 171(3): 557-572.e524.
74. Langfelder P, Horvath S. WGCNA: an R package for weighted correlation network analysis. *BMC Bioinformatics* 2008; 9(1): 559.
75. Zhang B, Horvath S. A general framework for weighted gene co-expression network analysis. *Stat Appl Genet Mol Biol* 2005; 4: Article17.

76. Zhang K, Wang M, Zhao Y, Wang W. Taiji: System-level identification of key transcription factors reveals transcriptional waves in mouse embryonic development. *Science Advances* 2019; 5(3): eaav3262.
77. Zhu Y, Chen Z, Zhang K, Wang M, Medovoy D, Whitaker JW et al. Constructing 3D interaction maps from 1D epigenomes. *Nat Commun* 2016; 7: 10812.
78. Bulik-Sullivan BK, Loh PR, Finucane HK, Ripke S, Yang J, Schizophrenia Working Group of the Psychiatric Genomics C et al. LD Score regression distinguishes confounding from polygenicity in genome-wide association studies. *Nat Genet* 2015; 47(3): 291-295.
79. Holloway T, Moreno JL, Umali A, Rayannavar V, Hodes GE, Russo SJ et al. Prenatal stress induces schizophrenia-like alterations of serotonin 2A and metabotropic glutamate 2 receptors in the adult offspring: role of maternal immune system. *J Neurosci* 2013; 33(3): 1088-1098.
80. Kim S, Kim H, Yim YS, Ha S, Atarashi K, Tan TG et al. Maternal gut bacteria promote neurodevelopmental abnormalities in mouse offspring. *Nature* 2017; 549(7673): 528-532.
81. Darnaudéry M, Dutriez I, Viltart O, Morley-Fletcher S, Maccari S. Stress during gestation induces lasting effects on emotional reactivity of the dam rat. *Behav Brain Res* 2004; 153(1): 211-216.
82. Vanbesien-Mailliot CC, Wolowczuk I, Mairesse J, Viltart O, Delacre M, Khalife J et al. Prenatal stress has pro-inflammatory consequences on the immune system in adult rats. *Psychoneuroendocrinology* 2007; 32(2): 114-124.
83. Ji F, Sadreyev RI. RNA-seq: Basic Bioinformatics Analysis. *Curr Protoc Mol Biol* 2018; 124(1): e68.
84. Wittkopp PJ, Kalay G. Cis-regulatory elements: molecular mechanisms and evolutionary processes underlying divergence. *Nat Rev Genet* 2011; 13(1): 59-69.
85. Jaster AM, Hadlock TM, Buzzi B, Maltman JL, Silva GM, Saha S et al. Sex-specific role of the 5-HT(2A) receptor in psilocybin-induced extinction of opioid reward. *Nat Commun* 2025; 16(1): 10206.
86. Creyghton MP, Cheng AW, Welstead GG, Kooistra T, Carey BW, Steine EJ et al. Histone H3K27ac separates active from poised enhancers and predicts developmental state. *Proc Natl Acad Sci U S A* 2010; 107(50): 21931-21936.

87. Moretto E, Murru L, Martano G, Sassone J, Passafaro M. Glutamatergic synapses in neurodevelopmental disorders. *Prog Neuropsychopharmacol Biol Psychiatry* 2018; 84(Pt B): 328-342.
88. Channer B, Matt SM, Nickoloff-Bybel EA, Pappa V, Agarwal Y, Wickman J et al. Dopamine, Immunity, and Disease. *Pharmacol Rev* 2023; 75(1): 62-158.
89. Perez J, Tardito D, Racagni G, Smeraldi E, Zanardi R. cAMP signaling pathway in depressed patients with psychotic features. *Molecular Psychiatry* 2002; 7(2): 208-212.
90. Sharova V, Ignatiuk V, Izvolskaia M, Zakharova L. Disruption of Intranasal GnRH Neuronal Migration Route into the Brain Induced by Proinflammatory Cytokine IL-6: Ex Vivo and In Vivo Rodent Models. *Int J Mol Sci* 2023; 24(21).
91. Morena M, Patel S, Bains JS, Hill MN. Neurobiological Interactions Between Stress and the Endocannabinoid System. *Neuropsychopharmacology* 2016; 41(1): 80-102.
92. Weinberger DR. Implications of normal brain development for the pathogenesis of schizophrenia. *Arch Gen Psychiatry* 1987; 44(7): 660-669.
93. Davis KL, Kahn RS, Ko G, Davidson M. Dopamine in schizophrenia: a review and reconceptualization. *Am J Psychiatry* 1991; 148(11): 1474-1486.
94. Lee DK, Cheng R, Nguyen T, Fan T, Kariyawasam AP, Liu Y et al. Characterization of apelin, the ligand for the APJ receptor. *J Neurochem* 2000; 74(1): 34-41.
95. Reaux A, De Mota N, Skultetyova I, Lenkei Z, El Messari S, Gallatz K et al. Physiological role of a novel neuropeptide, apelin, and its receptor in the rat brain. *J Neurochem* 2001; 77(4): 1085-1096.
96. Newson MJ, Pope GR, Roberts EM, Lolait SJ, O'Carroll AM. Stress-dependent and gender-specific neuroregulatory roles of the apelin receptor in the hypothalamic-pituitary-adrenal axis response to acute stress. *J Endocrinol* 2013; 216(1): 99-109.
97. Van Battum EY, Brignani S, Pasterkamp RJ. Axon guidance proteins in neurological disorders. *Lancet Neurol* 2015; 14(5): 532-546.
98. Matteoli M, Pozzi D, Fossati M, Menna E. Immune synaptopathies: how maternal immune activation impacts synaptic function during development. *Embo j* 2023; 42(13): e113796.
99. Funk AJ, McCullumsmith RE, Haroutunian V, Meador-Woodruff JH. Abnormal activity of the MAPK- and cAMP-associated signaling pathways in frontal cortical areas in postmortem brain in schizophrenia. *Neuropsychopharmacology* 2012; 37(4): 896-905.

100. Capellán R, Orihuel J, Marcos A, Ucha M, Moreno-Fernández M, Casquero-Veiga M *et al.* Interaction between maternal immune activation and peripubertal stress in rats: impact on cocaine addiction-like behaviour, morphofunctional brain parameters and striatal transcriptome. *Translational Psychiatry* 2023; 13(1): 84.
101. Mulder PA, Huisman S, Landlust AM, Moss J, Piening S, Hennekam RC *et al.* Development, behaviour and autism in individuals with SMC1A variants. *J Child Psychol Psychiatry* 2019; 60(3): 305-313.
102. Kranz TM, Goetz RR, Walsh-Messinger J, Goetz D, Antonius D, Dolgalev I *et al.* Rare variants in the neurotrophin signaling pathway implicated in schizophrenia risk. *Schizophr Res* 2015; 168(1-2): 421-428.
103. Del Puerto A, Lopez-Fonseca C, Simon-Garcia A, Martí-Prado B, Barrios-Munoz AL, Pose-Utrilla J *et al.* Kidins220 sets the threshold for survival of neural stem cells and progenitors to sustain adult neurogenesis. *Cell Death Dis* 2023; 14(8): 500.
104. Buxton DS, Batten DJ, Crofts JJ, Chuzhanova N. Predicting novel genomic regions linked to genetic disorders using GWAS and chromosome conformation data - a case study of schizophrenia. *Sci Rep* 2019; 9(1): 17940.
105. Yazdani A, Mendez-Giraldez R, Yazdani A, Kosorok MR, Roussos P. Differential gene regulatory pattern in the human brain from schizophrenia using transcriptomic-causal network. *BMC Bioinformatics* 2020; 21(1): 469.
106. Greene C, Hanley N, Campbell M. Blood-brain barrier associated tight junction disruption is a hallmark feature of major psychiatric disorders. *Translational Psychiatry* 2020; 10(1): 373.
107. Ng LF, Kaur P, Bunnag N, Suresh J, Sung ICH, Tan QH *et al.* WNT Signaling in Disease. *Cells* 2019; 8(8).
108. Zimmerberg B, Sageser KA. Comparison of Two Rodent Models of Maternal Separation on Juvenile Social Behavior. *Frontiers in Psychiatry* 2011; Volume 2 - 2011.
109. Grosz BR, Golovchenko NB, Ellis M, Kumar K, Nicholson GA, Antonellis A *et al.* A de novo EGR2 variant, c.1232A > G p.Asp411Gly, causes severe early-onset Charcot-Marie-Tooth Neuropathy Type 3 (Dejerine-Sottas Neuropathy). *Sci Rep* 2019; 9(1): 19336.
110. Cali E, Suri M, Scala M, Ferla MP, Alavi S, Faqeih EA *et al.* Biallelic PRMT7 pathogenic variants are associated with a recognizable syndromic neurodevelopmental disorder with short stature, obesity, and craniofacial and digital abnormalities. *Genet Med* 2023; 25(1): 135-142.

111. Liu Z, Deng C, Zhou Z, Xiao Y, Jiang S, Zhu B *et al.* Epigenomic tomography for probing spatially defined chromatin state in the brain. *Cell Rep Methods* 2024; 4(3): 100738.
112. Naler LB, Hsieh YP, Geng S, Zhou Z, Li L, Lu C. Epigenomic and transcriptomic analyses reveal differences between low-grade inflammation and severe exhaustion in LPS-challenged murine monocytes. *Commun Biol* 2022; 5(1): 102.
113. Meyer EE, Clancy CE, Lewis TJ. Dynamics of adrenergic signaling in cardiac myocytes and implications for pharmacological treatment. *J Theor Biol* 2021; 519: 110619.
114. Hollins SL, Zavitsanou K, Walker FR, Cairns MJ. Alteration of imprinted Dlk1-Dio3 miRNA cluster expression in the entorhinal cortex induced by maternal immune activation and adolescent cannabinoid exposure. *Transl Psychiatry* 2014; 4(9): e452.
115. Kent LN, Rumi MA, Kubota K, Lee DS, Soares MJ. FOSL1 is integral to establishing the maternal-fetal interface. *Mol Cell Biol* 2011; 31(23): 4801-4813.
116. Langfelder P, Horvath S. WGCNA: an R package for weighted correlation network analysis. *BMC Bioinformatics* 2008; 9: 559.
117. Keever MR, Zhang P, Bolt CR, Antonson AM, Rymut HE, Caputo MP *et al.* Lasting and Sex-Dependent Impact of Maternal Immune Activation on Molecular Pathways of the Amygdala. *Front Neurosci* 2020; 14: 774.
118. Rodriguez-Zas SL, Nowak RA, Antonson AM, Rund L, Bhamidi S, Gomez AN *et al.* Immune and metabolic challenges induce changes in pain sensation and related pathways in the hypothalamus. *Physiol Genomics* 2024; 56(4): 343-359.
119. Wu P, Liu Z, Zheng L, Du Y, Zhou Z, Wang W *et al.* Comprehensive multimodal and multiomic profiling reveals epigenetic and transcriptional reprogramming in lung tumors. *Commun Biol* 2025; 8(1): 527.
120. Li M, Santpere G, Imamura Kawasawa Y, Evgrafov OV, Gulden FO, Pochareddy S *et al.* Integrative functional genomic analysis of human brain development and neuropsychiatric risks. *Science* 2018; 362(6420).
121. Hashimoto R, Ohi K, Yasuda Y, Fukumoto M, Yamamori H, Takahashi H *et al.* Variants of the RELA gene are associated with schizophrenia and their startle responses. *Neuropsychopharmacology* 2011; 36(9): 1921-1931.
122. Kanehisa M, Goto S. KEGG: Kyoto Encyclopedia of Genes and Genomes. *Nucleic Acids Research* 2000; 28(1): 27-30.

123. Hu TM, Chen CH, Chuang YA, Hsu SH, Cheng MC. Resequencing of early growth response 2 (EGR2) gene revealed a recurrent patient-specific mutation in schizophrenia. *Psychiatry Res* 2015; 228(3): 958-960.
124. Griffin EN, Jucius T, Sim SE, Harris BS, Heinz S, Ackerman SL. RREB1 regulates neuronal proteostasis and the microtubule network. *Sci Adv* 2024; 10(2): eadh3929.
125. Comes AL, Czamara D, Adorjan K, Anderson-Schmidt H, Andlauer TFM, Budde M *et al.* The role of environmental stress and DNA methylation in the longitudinal course of bipolar disorder. *Int J Bipolar Disord* 2020; 8(1): 9.
126. Montano C, Taub MA, Jaffe A, Briem E, Feinberg JI, Trygvadottir R *et al.* Association of DNA Methylation Differences With Schizophrenia in an Epigenome-Wide Association Study. *JAMA Psychiatry* 2016; 73(5): 506-514.
127. Uffelmann E, Huang QQ, Munung NS, de Vries J, Okada Y, Martin AR *et al.* Genome-wide association studies. *Nature Reviews Methods Primers* 2021; 1(1): 59.
128. Buniello A, MacArthur JAL, Cerezo M, Harris LW, Hayhurst J, Malangone C *et al.* The NHGRI-EBI GWAS Catalog of published genome-wide association studies, targeted arrays and summary statistics 2019. *Nucleic Acids Res* 2019; 47(D1): D1005-d1012.
129. Collins AL, Sullivan PF. Genome-wide association studies in psychiatry: what have we learned? *Br J Psychiatry* 2013; 202(1): 1-4.
130. Reisinger S, Khan D, Kong E, Berger A, Pollak A, Pollak DD. The Poly(I:C)-induced maternal immune activation model in preclinical neuropsychiatric drug discovery. *Pharmacology & Therapeutics* 2015; 149: 213-226.
131. Bulik-Sullivan BK, Loh P-R, Finucane HK, Ripke S, Yang J, Patterson N *et al.* LD Score regression distinguishes confounding from polygenicity in genome-wide association studies. *Nature Genetics* 2015; 47(3): 291-295.
132. Villar D, Berthelot C, Aldridge S, Rayner Tim F, Lukk M, Pignatelli M *et al.* Enhancer Evolution across 20 Mammalian Species. *Cell* 2015; 160(3): 554-566.
133. Lickwar CR, Camp JG, Weiser M, Cocchiaro JL, Kingsley DM, Furey TS *et al.* Genomic dissection of conserved transcriptional regulation in intestinal epithelial cells. *PLOS Biology* 2017; 15(8): e2002054.
134. Demontis D, Walters RK, Martin J, Mattheisen M, Als TD, Agerbo E *et al.* Discovery of the first genome-wide significant risk loci for attention deficit/hyperactivity disorder. *Nat Genet* 2019; 51(1): 63-75.

135. Jansen IE, Savage JE, Watanabe K, Bryois J, Williams DM, Steinberg S *et al.* Genome-wide meta-analysis identifies new loci and functional pathways influencing Alzheimer's disease risk. *Nature Genetics* 2019; 51(3): 404-413.
136. Grove J, Ripke S, Als TD, Mattheisen M, Walters RK, Won H *et al.* Identification of common genetic risk variants for autism spectrum disorder. *Nat Genet* 2019; 51(3): 431-444.
137. Ruderfer DM, Fanous AH, Ripke S, McQuillin A, Amdur RL, Gejman PV *et al.* Polygenic dissection of diagnosis and clinical dimensions of bipolar disorder and schizophrenia. *Mol Psychiatry* 2014; 19(9): 1017-1024.
138. Howson JMM, Zhao W, Barnes DR, Ho WK, Young R, Paul DS *et al.* Fifteen new risk loci for coronary artery disease highlight arterial-wall-specific mechanisms. *Nat Genet* 2017; 49(7): 1113-1119.
139. Nagel M, Jansen PR, Stringer S, Watanabe K, de Leeuw CA, Bryois J *et al.* Meta-analysis of genome-wide association studies for neuroticism in 449,484 individuals identifies novel genetic loci and pathways. *Nature Genetics* 2018; 50(7): 920-927.
140. Lam M, Chen C-Y, Li Z, Martin AR, Bryois J, Ma X *et al.* Comparative genetic architectures of schizophrenia in East Asian and European populations. *Nature Genetics* 2019; 51(12): 1670-1678.
141. Bale TL, Baram TZ, Brown AS, Goldstein JM, Insel TR, McCarthy MM *et al.* Early Life Programming and Neurodevelopmental Disorders. *Biological Psychiatry* 2010; 68(4): 314-319.
142. Glover V, O'Connor TG, O'Donnell K. Prenatal stress and the programming of the HPA axis. *Neuroscience & Biobehavioral Reviews* 2010; 35(1): 17-22.
143. Fox SE, Levitt P, Nelson CA, 3rd. How the timing and quality of early experiences influence the development of brain architecture. *Child Dev* 2010; 81(1): 28-40.
144. Meaney MJ. Maternal care, gene expression, and the transmission of individual differences in stress reactivity across generations. *Annu Rev Neurosci* 2001; 24: 1161-1192.
145. Mirabella F, Desiato G, Mancinelli S, Fossati G, Rasile M, Morini R *et al.* Prenatal interleukin 6 elevation increases glutamatergic synapse density and disrupts hippocampal connectivity in offspring. *Immunity* 2021; 54(11): 2611-2631.e2618.

146. Elgueta D, Murgas P, Riquelme E, Yang G, Cancino GI. Consequences of Viral Infection and Cytokine Production During Pregnancy on Brain Development in Offspring. *Front Immunol* 2022; 13: 816619.
147. Choi GB, Yim YS, Wong H, Kim S, Kim H, Kim SV *et al.* The maternal interleukin-17a pathway in mice promotes autism-like phenotypes in offspring. *Science* 2016; 351(6276): 933-939.
148. Brown AS, Hooton J, Schaefer CA, Zhang H, Petkova E, Babulas V *et al.* Elevated maternal interleukin-8 levels and risk of schizophrenia in adult offspring. *Am J Psychiatry* 2004; 161(5): 889-895.
149. Gilmore JH, Fredrik Jarskog L, Vadlamudi S, Lauder JM. Prenatal infection and risk for schizophrenia: IL-1beta, IL-6, and TNFalpha inhibit cortical neuron dendrite development. *Neuropsychopharmacology* 2004; 29(7): 1221-1229.
150. Rudolph MD, Graham AM, Feczko E, Miranda-Dominguez O, Rasmussen JM, Nardos R *et al.* Maternal IL-6 during pregnancy can be estimated from newborn brain connectivity and predicts future working memory in offspring. *Nat Neurosci* 2018; 21(5): 765-772.
151. Meyer U, Murray PJ, Urwyler A, Yee BK, Schedlowski M, Feldon J. Adult behavioral and pharmacological dysfunctions following disruption of the fetal brain balance between pro-inflammatory and IL-10-mediated anti-inflammatory signaling. *Mol Psychiatry* 2008; 13(2): 208-221.
152. Aguilar-Valles A, Rodrigue B, Matta-Camacho E. Maternal Immune Activation and the Development of Dopaminergic Neurotransmission of the Offspring: Relevance for Schizophrenia and Other Psychoses. *Front Psychiatry* 2020; 11: 852.
153. DeRosa H, Caradonna SG, Tran H, Marrocco J, Kentner AC. Got milk? Maternal immune activation during the mid-lactational period affects nutritional milk quality and adolescent offspring sensory processing in male and female rats. *Molecular Psychiatry* 2022; 27(12): 4829-4842.
154. You P, Sui J, Jin Z, Huang L, Wei H, Xu Q. Interaction between maternal immune activation and postpartum immune stress in neuropsychiatric phenotypes. *Behavioural Brain Research* 2024; 469: 115049.
155. Lupien SJ, McEwen BS, Gunnar MR, Heim C. Effects of stress throughout the lifespan on the brain, behaviour and cognition. *Nature Reviews Neuroscience* 2009; 10(6): 434-445.
156. Li W, Chen M, Feng X, Song M, Shao M, Yang Y *et al.* Maternal immune activation alters adult behavior, intestinal integrity, gut microbiota and the gut inflammation. *Brain Behav* 2021; 11(5): e02133.

157. Sokol DK, Maloney B, Westmark CJ, Lahiri DK. Novel Contribution of Secreted Amyloid-beta Precursor Protein to White Matter Brain Enlargement in Autism Spectrum Disorder. *Front Psychiatry* 2019; 10: 165.
158. Chen J, Dong X, Cheng X, Zhu Q, Zhang J, Li Q *et al.* Ogt controls neural stem/progenitor cell pool and adult neurogenesis through modulating Notch signaling. *Cell Reports* 2021; 34(13): 108905.
159. Gutierrez H, Davies AM. Regulation of neural process growth, elaboration and structural plasticity by NF-κB. *Trends Neurosci* 2011; 34(6): 316-325.
160. Fabbri C, Serretti A. Role of 108 schizophrenia-associated loci in modulating psychopathological dimensions in schizophrenia and bipolar disorder. *Am J Med Genet B Neuropsychiatr Genet* 2017; 174(7): 757-764.
161. Han Q, Sun Y-A, Zong Y, Chen C, Wang H-F, Tan L *et al.* Common Variants in PLXNA4 and Correlation to CSF-related Phenotypes in Alzheimer's Disease. *Frontiers in Neuroscience* 2018; 12.
162. Ravindran E, Hu H, Yuzwa SA, Hernandez-Miranda LR, Kraemer N, Ninnemann O *et al.* Homozygous ARHGEF2 mutation causes intellectual disability and midbrain-hindbrain malformation. *PLoS Genet* 2017; 13(4): e1006746.
163. Richetto J, Chesters R, Cattaneo A, Labouesse MA, Gutierrez AMC, Wood TC *et al.* Genome-Wide Transcriptional Profiling and Structural Magnetic Resonance Imaging in the Maternal Immune Activation Model of Neurodevelopmental Disorders. *Cerebral Cortex* 2016; 27(6): 3397-3413.
164. Salazar JL, Yang SA, Lin YQ, Li-Kroeger D, Marcogliese PC, Deal SL *et al.* TM2D genes regulate Notch signaling and neuronal function in Drosophila. *PLoS Genet* 2021; 17(12): e1009962.
165. Silbereis John C, Pochareddy S, Zhu Y, Li M, Sestan N. The Cellular and Molecular Landscapes of the Developing Human Central Nervous System. *Neuron* 2016; 89(2): 248-268.
166. Tau GZ, Peterson BS. Normal Development of Brain Circuits. *Neuropsychopharmacology* 2010; 35(1): 147-168.
167. Santos-Toscano R, Borcel É, Ucha M, Orihuel J, Capellán R, Roura-Martínez D *et al.* Unaltered cocaine self-administration in the prenatal LPS rat model of schizophrenia. *Progress in Neuro-Psychopharmacology and Biological Psychiatry* 2016; 69: 38-48.

168. Henricks AM, Sullivan EDK, Dwiel LL, Li JY, Wallin DJ, Khokhar JY *et al.* Maternal immune activation and adolescent alcohol exposure increase alcohol drinking and disrupt cortical-striatal-hippocampal oscillations in adult offspring. *Translational Psychiatry* 2022; 12(1): 288.
169. Caspi A, Moffitt TE. Gene–environment interactions in psychiatry: joining forces with neuroscience. *Nature Reviews Neuroscience* 2006; 7(7): 583-590.
170. Bilbo SD, Schwarz JM. Early-life programming of later-life brain and behavior: a critical role for the immune system. *Front Behav Neurosci* 2009; 3: 14.
171. Bilbo SD. Early-life infection is a vulnerability factor for aging-related glial alterations and cognitive decline. *Neurobiol Learn Mem* 2010; 94(1): 57-64.
172. Meyer U. Neurodevelopmental Resilience and Susceptibility to Maternal Immune Activation. *Trends Neurosci* 2019; 42(11): 793-806.
173. Smith KE, Pollak SD. Early life stress and development: potential mechanisms for adverse outcomes. *Journal of Neurodevelopmental Disorders* 2020; 12(1): 34.
174. Birnie MT, Baram TZ. The evolving neurobiology of early-life stress. *Neuron* 2025; 113(10): 1474-1490.
175. Ikezu S, Yeh H, Delpech J-C, Woodbury ME, Van Enoo AA, Ruan Z *et al.* Inhibition of colony stimulating factor 1 receptor corrects maternal inflammation-induced microglial and synaptic dysfunction and behavioral abnormalities. *Molecular Psychiatry* 2021; 26(6): 1808-1831.
176. Vermeij WP, Dollé ME, Reiling E, Jaarsma D, Payan-Gomez C, Bombardieri CR *et al.* Restricted diet delays accelerated ageing and genomic stress in DNA-repair-deficient mice. *Nature* 2016; 537(7620): 427-431.
177. Reemst K, Kracht L, Kotah JM, Rahimian R, van Irsen AAS, Congrains Sotomayor G *et al.* Early-life stress lastingly impacts microglial transcriptome and function under basal and immune-challenged conditions. *Translational Psychiatry* 2022; 12(1): 507.
178. Kotah JM, Kater MSJ, Brosens N, Lesuis SL, Tandari R, Blok TM *et al.* Early-life stress and amyloidosis in mice share pathogenic pathways involving synaptic mitochondria and lipid metabolism. *Alzheimers Dement* 2024; 20(3): 1637-1655.
179. McEwen BS, Akil H. Revisiting the Stress Concept: Implications for Affective Disorders. *The Journal of Neuroscience* 2020; 40(1): 12-21.

180. Carrier M, Dolhan K, Bobotis BC, Desjardins M, Tremblay M. The implication of a diversity of non-neuronal cells in disorders affecting brain networks. *Front Cell Neurosci* 2022; 16: 1015556.
181. Sekar A, Bialas AR, de Rivera H, Davis A, Hammond TR, Kamitaki N et al. Schizophrenia risk from complex variation of complement component 4. *Nature* 2016; 530(7589): 177-183.
182. Salter MW, Stevens B. Microglia emerge as central players in brain disease. *Nature Medicine* 2017; 23(9): 1018-1027.
183. Russo SJ, Murrough JW, Han M-H, Charney DS, Nestler EJ. Neurobiology of resilience. *Nature Neuroscience* 2012; 15(11): 1475-1484.
184. Southwick SM, Charney DS. The science of resilience: implications for the prevention and treatment of depression. *Science* 2012; 338(6103): 79-82.

Acknowledgements

The study was supported by the United States National Institutes of Health grants R01DA056187 (to C.L.), R01MH084894 (to J.G.-M.), F30MH116550 (to J.M.S), and by CRIPT (Center for Research on Influenza Pathogenesis and Transmission), an NIAID funded Center of Excellence for Influenza Research and Response (CEIRR, contract # 75N93021C00014, to A.G.-S.).

Author Contributions

J.G.-M. and C.L. conceived the study. B.Z. performed all ChIP-seq and RNA-seq experiments and conducted initial data analysis. G.L. conducted the bioinformatics analysis. J.M.S. performed the animal experiments and tissue dissections. T.M.H. and C.W. contributed to data analysis. A.G.-S. provided the influenza virus. J.G.-M. contributed to data interpretation. G.L., C.L., B.Z., and J.G.-M. wrote the manuscript. All authors proofread the manuscript and provided feedback.

Competing Interests

The A.G.-S. laboratory has received research support from Avimex, Dynavax, Pharmamar, 7Hills Pharma, ImmunityBio and Accurius, outside of the reported work. A.G.-S. has consulting agreements for the following companies involving cash and/or stock: Castlevax, Amovir, Vivaldi Biosciences, Contraflect, 7Hills Pharma, Avimex, Pagoda, Accurius, Esperovax, Applied Biological Laboratories, Pharmamar, CureLab Oncology, CureLab Veterinary, Synairgen, Paratus, Pfizer, Virofend and Prosetta, outside of the reported work. A.G.-S. has been an invited speaker in meeting events organized by Seqirus, Janssen, Abbott, Astrazeneca and Novavax. A.G.-S. is an inventor on patents and patent applications on the use of antivirals and vaccines for the treatment and prevention of virus infections and cancer, owned by the Icahn School of Medicine at Mount Sinai, New York, outside of the reported work. J.G.-M. has received research support from Noetic Fund, Terran Biosciences, and Gonogo Solutions. All other authors declare no competing interests.

ADDITIONAL INFORMATION

Supplementary information

The online version contains supplementary material available at...

Correspondence and requests for materials should be addressed to Javier González-Maeso and Chang Lu.

ARTICLE IN PRESS

Figures Captions

Figure 1 MIA and cross-fostering design. N = 6 mice per group (A to D).

Pregnant dams were administered either saline (Mock) or influenza virus (MIA) to induce maternal immune activation. Offspring were subsequently assigned to four experimental groups based on prenatal and postnatal exposure: Group A, Mock-Mock; Group B, MIA-Mock; Group C, Mock-MIA; and Group D, MIA-MIA. Arrows indicate the grouping process and treatment combinations across developmental stages. Created with BioRender.com.

Figure 2 Prenatal effects of MIA on offspring epigenetic and transcriptomic profiles.

- a, Bar plots showing the numbers of differential enhancers/promoters and DEGs with increased (red) or decreased (gray) intensity in MIA-Mock vs. Mock-Mock (left) and MIA-MIA vs. Mock-MIA (right) comparisons.
- b, Venn diagrams showing the overlap between DEGs, differential promoter-linked genes, and differential enhancer-linked genes in each comparison.
- c, Top 20 KEGG pathways enriched among genes involving both transcriptomic and epigenomic (either in promoter or enhancer) changes in the MIA-Mock vs. Mock-Mock comparison.
- d, Top 20 KEGG pathways enriched among genes involving both transcriptomic and epigenomic (either in promoter or enhancer) changes in the MIA-MIA vs. Mock-MIA comparison. Dot size reflects the number of genes per pathway; color scale indicates fold enrichment; significance is shown as $-\log_{10}(\text{FDR})$, with FDR < 0.05 used as the cutoff.

Figure 3 Shared and unique biological pathways altered by prenatal and postnatal effects of MIA based on differential enhancer-linked genes.

- a, Top 20 KEGG pathways enriched among genes linked to differential enhancers shared between the prenatal comparisons (MIA-Mock vs. Mock-Mock and MIA-MIA vs. Mock-MIA).
- b, Top 20 KEGG pathways enriched among genes linked to differential enhancers shared between the postnatal comparisons (Mock-MIA vs. Mock-Mock and MIA-MIA vs. MIA-Mock).
- c, Top 20 GO pathways uniquely enriched among genes linked to differential enhancers in the prenatal comparisons (MIA-Mock vs. Mock-Mock and MIA-MIA vs. Mock-MIA), representing biological processes more prominently associated with prenatal MIA exposure.
- d, Top 20 GO pathways uniquely enriched among genes linked to differential enhancers in the postnatal comparisons, representing biological processes more prominently associated with postnatal MIA exposure. Dot size indicates the number of genes per pathway; color scale indicates fold enrichment; significance is shown as $-\log_{10}(\text{FDR})$, with FDR < 0.05 used as the cutoff.

Figure 4 Postnatal effects of MIA on offspring epigenetic and transcriptomic profiles.

- a, Bar plots showing the numbers of differential enhancers/promoters and DEGs with increased (red) or decreased (gray) intensity in Mock-MIA vs. Mock-Mock (left) and MIA-Mock vs. MIA-MIA (right) comparisons.
- b, Venn diagrams showing the overlap between DEGs, differential promoter-linked genes, and differential enhancer-linked genes in each comparison.
- c, Top 20 KEGG pathways enriched among genes involving both transcriptomic and epigenomic (either in promoter or enhancer) changes in the Mock-MIA vs. Mock-Mock comparison.
- d, Top 20 KEGG pathways enriched among genes involving both transcriptomic and epigenomic (either in promoter or enhancer) changes in the MIA-Mock vs. MIA-MIA comparison.

Dot size indicates the number of genes per pathway; color scale indicates fold enrichment; significance is shown as $-\log_{10}(\text{FDR})$, with $\text{FDR} < 0.05$ used as the cutoff.

Figure 5 Differentially regulated transcription factor activity and target gene pathways altered by prenatal and postnatal MIA exposure.

a, Heatmap showing transcription factors differentially regulated between MIA-Mock and Mock-Mock, along with the top 20 KEGG pathways enriched among the regulated genes of these transcription factors.

b, Heatmap showing transcription factors differentially regulated between MIA-MIA and Mock-MIA, along with the top 20 KEGG pathways enriched among the regulated genes of these transcription factors.

c, Heatmap showing transcription factors differentially regulated between Mock-MIA and Mock-Mock, along with the top 20 KEGG pathways enriched among the regulated genes of these transcription factors.

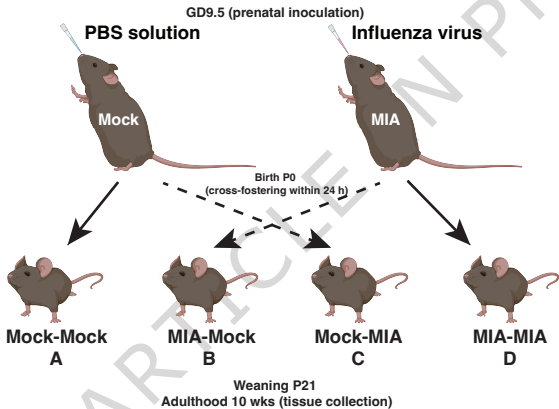
d, Heatmap showing transcription factors differentially regulated between MIA-MIA and MIA-Mock, along with the top 20 KEGG pathways enriched among the regulated genes of these transcription factors.

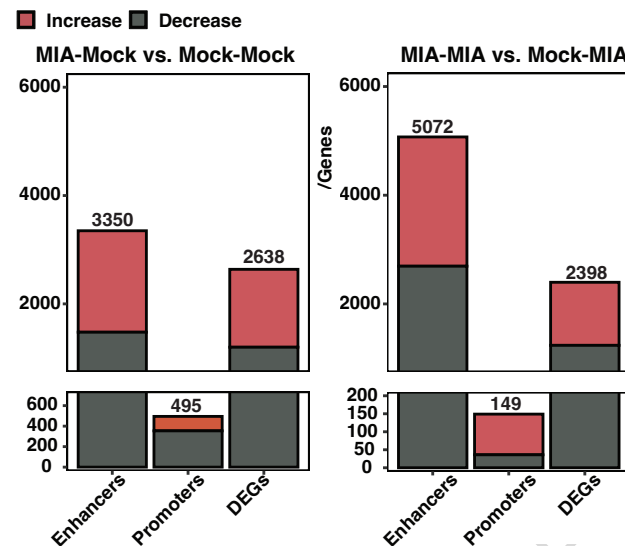
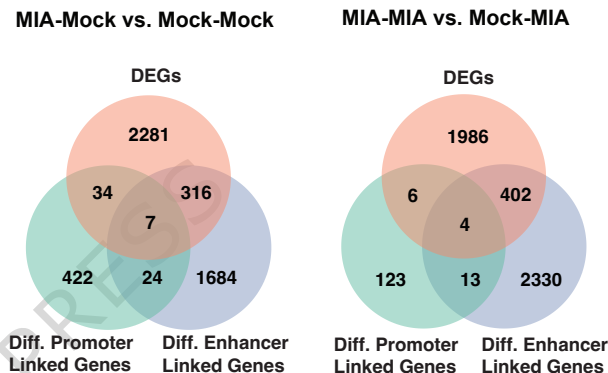
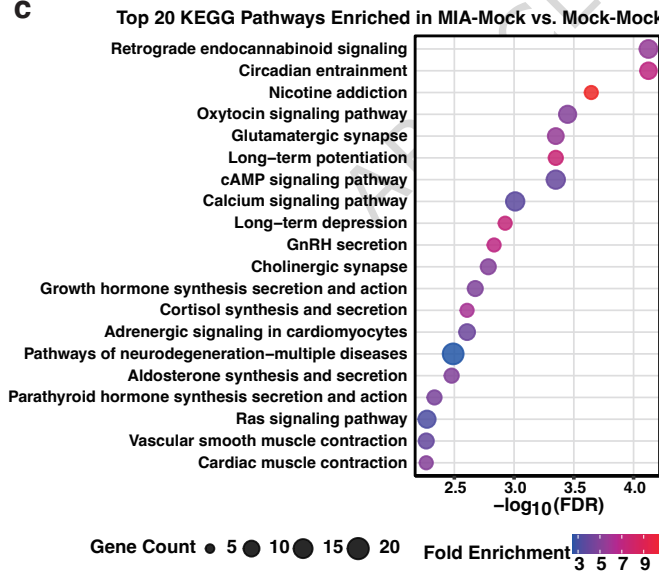
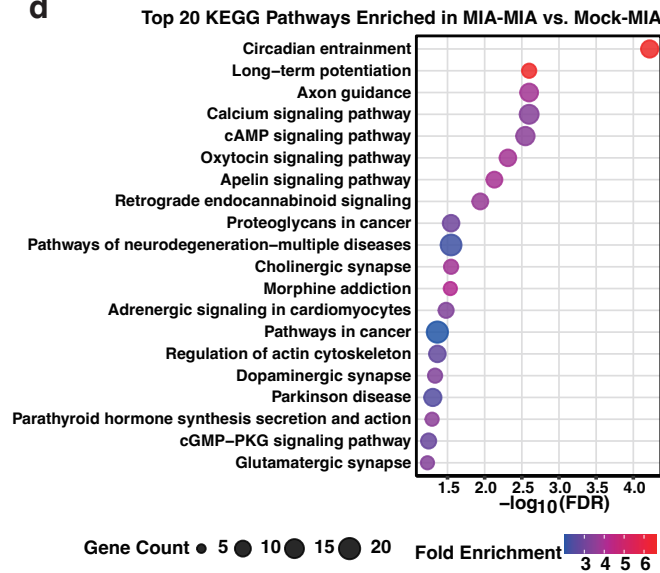
Heatmap values represent z-scores of PRP-normalized TF activity. Dot size reflects the number of regulated genes per pathway; color scale indicates fold enrichment; significance is shown as $-\log_{10}(\text{FDR})$, with $\text{FDR} < 0.05$ used as the cutoff.

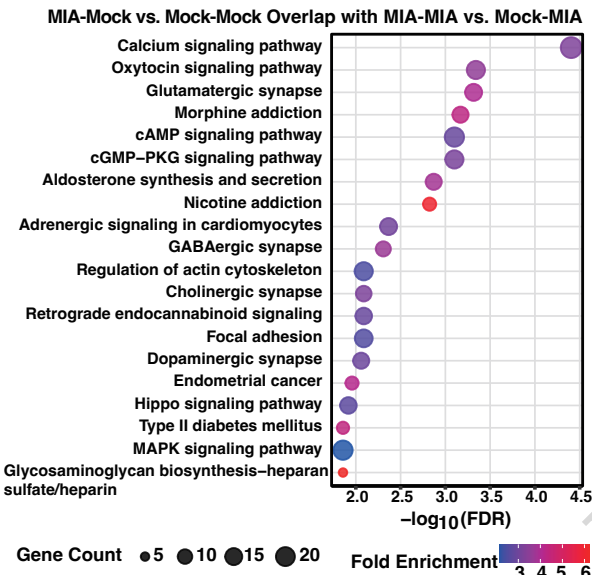
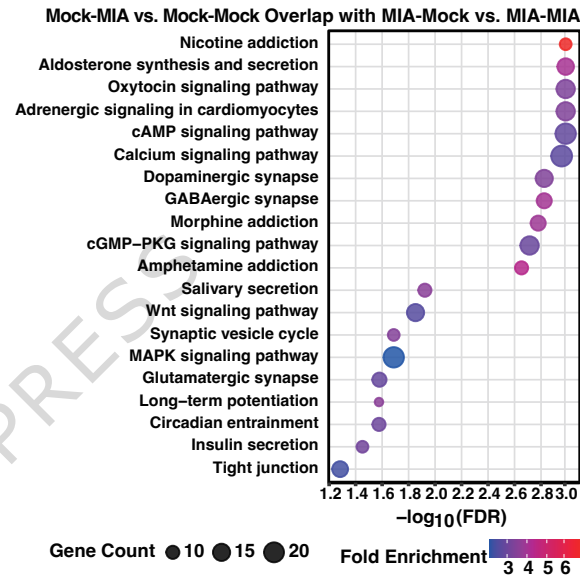
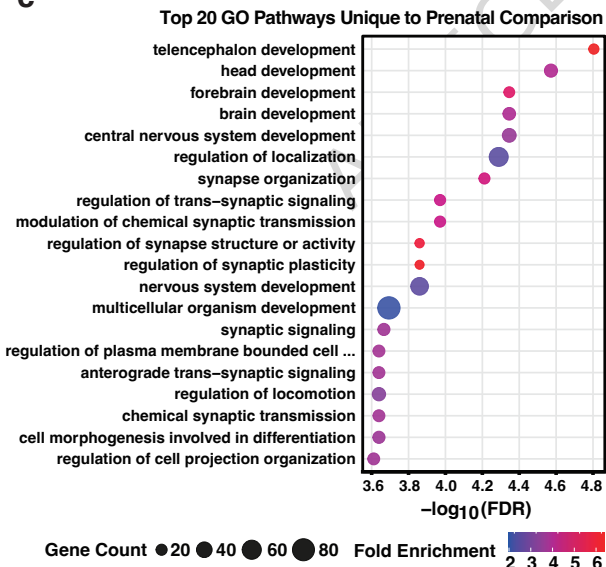
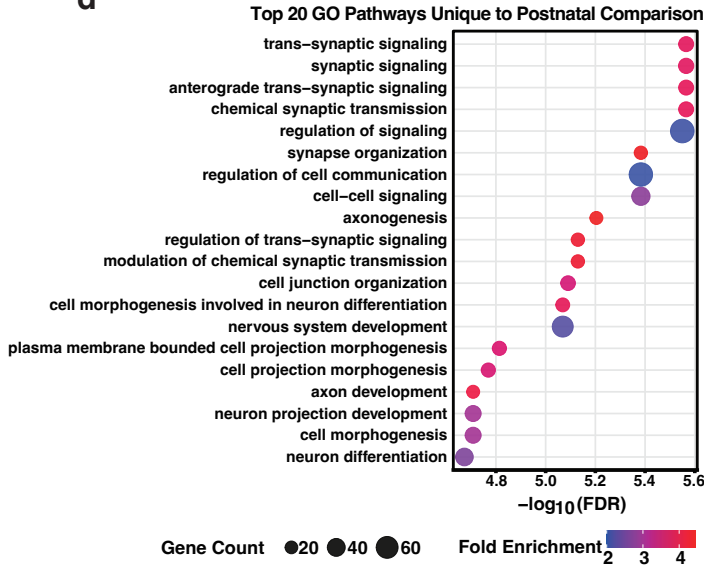
Figure 6 Enrichment of differential enhancer and promoter regions at disease-associated GWAS loci following maternal immune activation (MIA).

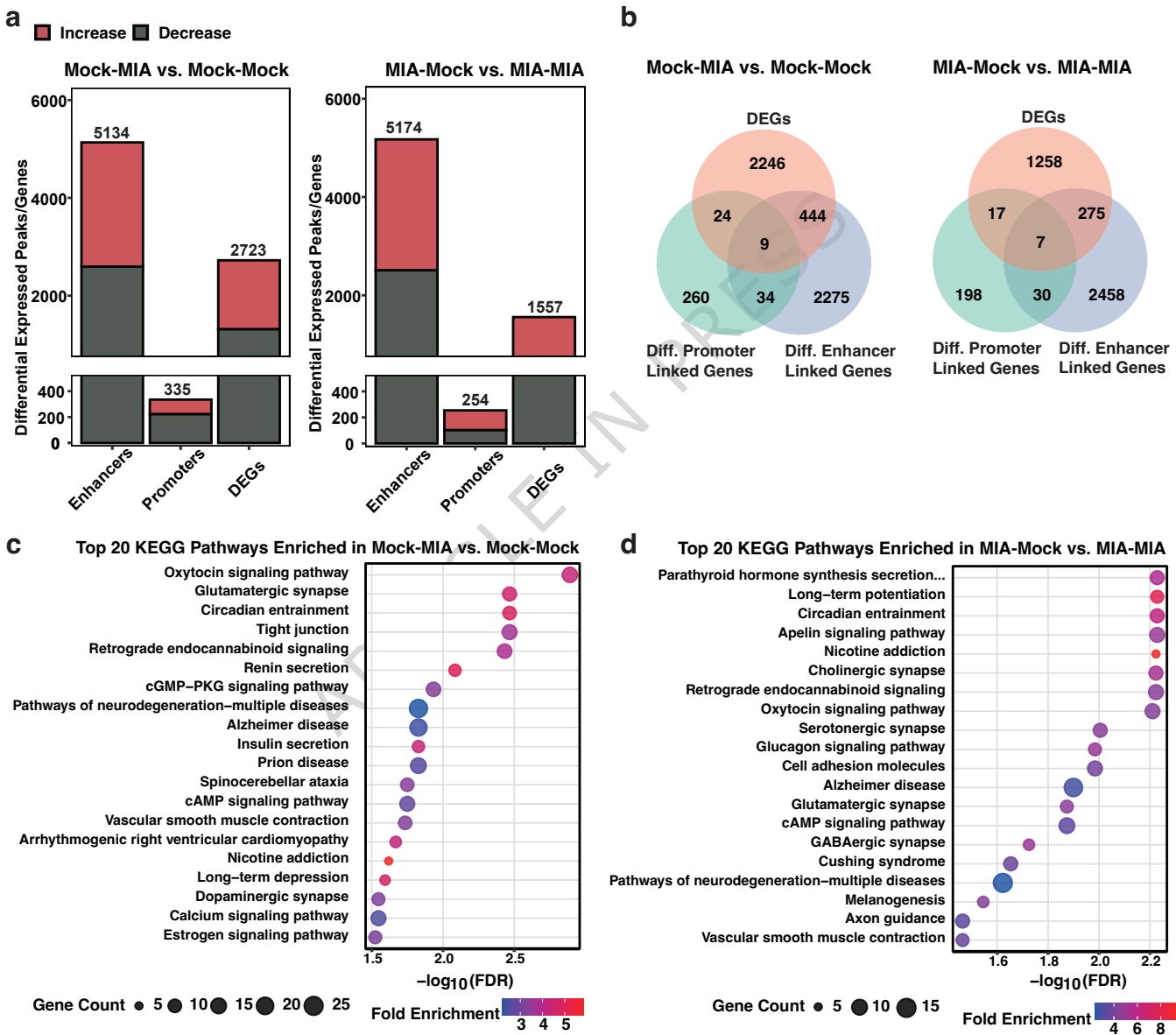
a, Heatmap showing $-\log_{10}(P)$ values for enrichment of differential enhancer regions at GWAS loci associated with neuropsychiatric and other disorders across all experimental comparisons.

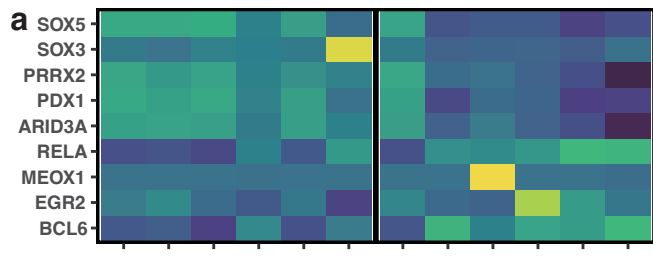
b, Heatmap showing $-\log_{10}(P)$ values for enrichment of differential promoter regions at GWAS loci associated with neuropsychiatric and other disorders across all experimental comparisons.



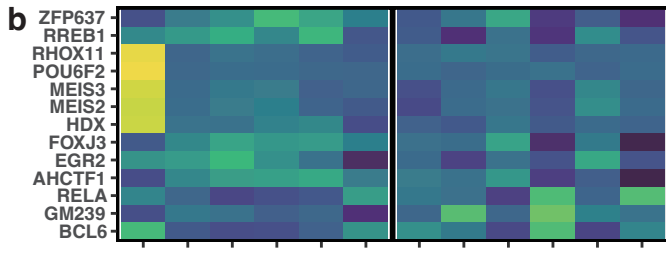
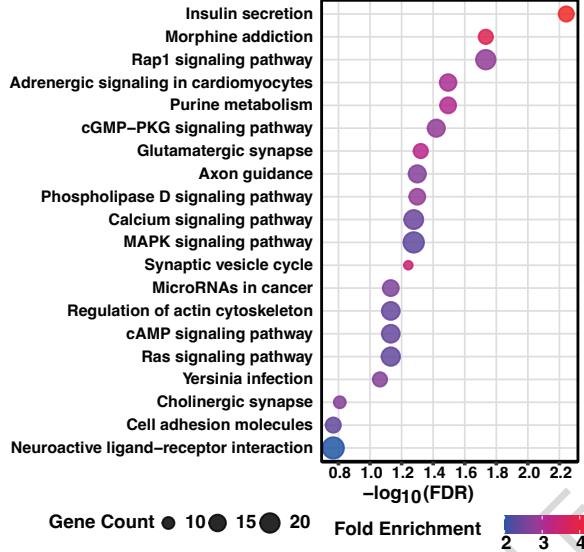
a**b****c****d**

a**b****c****d**

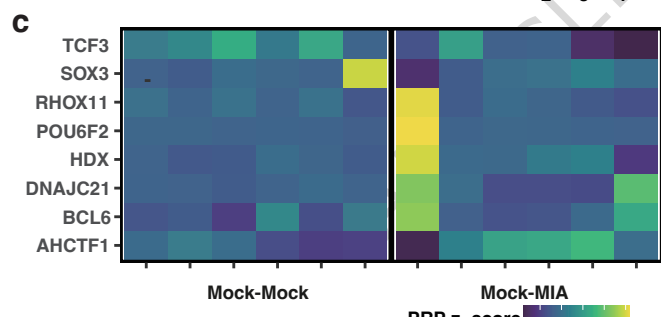
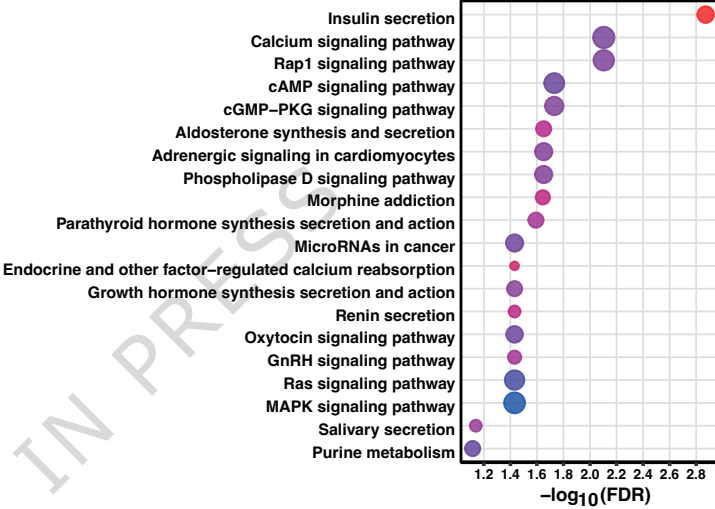




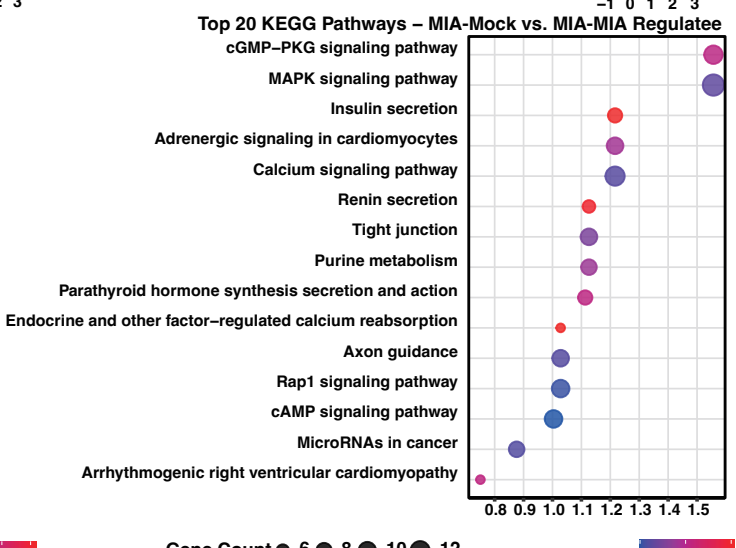
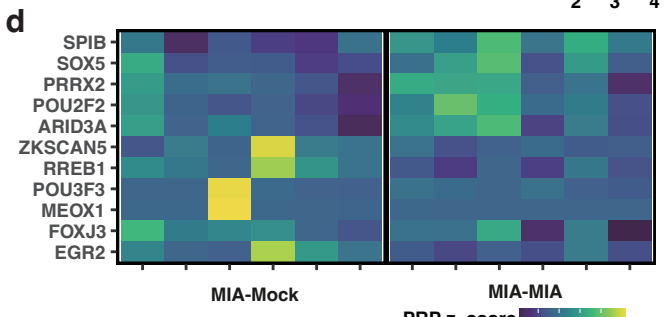
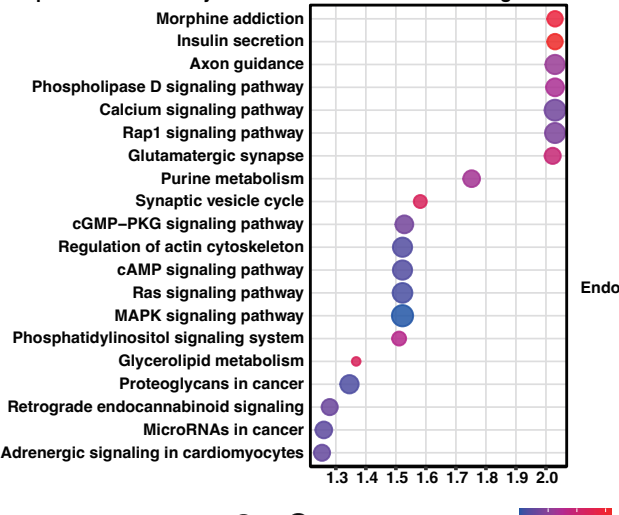
Top 20 KEGG Pathways – MIA-Mock vs. Mock-Mock Regulate

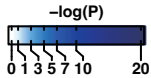


Top 20 KEGG Pathways – Mock-MIA vs. MIA-MIA Regulate



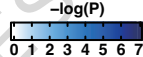
Top 20 KEGG Pathways – Mock-MIA vs. Mock-Mock Regulate



a

	Prenatal	Postnatal	No MIA
Schizophrenia	13.6	14.9	20.1
Bipolar Disorder	4.9	5.9	6.3
Depression	3.9	4.3	7.4
Neuroticism	3.7	4.9	7.6
Autism	2.6	2.6	2.8
Coronary Artery Disease	2.8	2.8	2.2
ADHD	2.9	2.1	3.2
Crohns Disease	2.0	3.0	1.9
Alzheimers	1.0	3.2	1.7
ALS	0.4	1.2	1.1
Type2 Diabetes	0.8	0.9	0.5
Ulcerative Colitis	1.2	1.7	0.2
Epilepsy	0.2	0.3	0.6
Celiac	0.4	0.0	0.3

MIA-Mock vs. Mock-Mock
MIA-MIA vs. Mock-MIA
Mock-MIA vs. Mock-Mock
MIA-Mock vs. MIA-MIA
Mock-Mock_1 vs. Mock-Mock_3
Mock-Mock_2 vs. Mock-Mock_1
Mock-Mock_2 vs. Mock-Mock_3

b

	Prenatal	Postnatal	No MIA
Schizophrenia	2.9	1.5	1.3
Neuroticism	1.1	1.5	0.2
Bipolar Disorder	2.2	1.0	1.9
Alzheimers	2.0	0.8	1.3
Coronary Artery Disease	0.8	1.6	0.9
Crohns Disease	1.6	0.4	1.1
Ulcerative Colitis	1.2	0.8	1.1
ALS	1.1	0.9	0.6
ADHD	0.6	0.5	1.4
Autism	0.4	0.3	1.3
Depression	0.1	0.5	0.9
Type2 Diabetes	0.2	1.0	0.3
Celiac	0.2	0.1	1.4
Epilepsy	0.7	0.3	0.5

MIA-Mock vs. Mock-Mock
MIA-MIA vs. Mock-MIA
Mock-MIA vs. Mock-Mock
MIA-Mock vs. MIA-MIA
Mock-Mock_1 vs. Mock-Mock_3
Mock-Mock_2 vs. Mock-Mock_1
Mock-Mock_2 vs. Mock-Mock_3